

INSTITUTO UNIVERSITÁRIO EGAS MONIZ

MESTRADO INTEGRADO EM MEDICINA DENTÁRIA

A AVALIAÇÃO DO IMPACTO DO CBCT NO DIAGNÓSTICO E MANEJO DAS PATOLOGIAS DOS SEIOS MAXILARES

Trabalho submetido por

Arthur Clevenot-Roux

para a obtenção do grau de Mestre em Medicina Dentária

junho de 2025

INSTITUTO UNIVERSITÁRIO EGAS MONIZ

MESTRADO INTEGRADO EM MEDICINA DENTÁRIA

A AVALIAÇÃO DO IMPACTO DO CBCT NO DIAGNÓSTICO E MANEJO DAS PATOLOGIAS DOS SEIOS MAXILARES

Trabalho submetido por

Arthur Clevenot-Roux

para a obtenção do grau de Mestre em Medicina Dentária

Trabalho orientado por

Prof. Doutor Gonçalo Martins Pereira

junho de 2025

AGRADECIMENTOS

Em primeiro lugar, gostaria de agradecer, com enorme gratidão ao Instituto Universitário Egas Moniz, School of Health and Science, por me ter a oportunidade de realizar os estudos que sempre quis fazer.

Um grande agradeço também ao meu orientador, Professor Doutor Gonçalo Martins Pereira pelo seu acompanhamento, disponibilidade, apoio e capacidade de resposta ao longo de toda esta tese.

Je souhaiterais remercier également ma mère, mon père et mon frère de m'avoir permis de réaliser ces études ici au Portugal. Sans eux cela n'aura pas pu être possible. Merci pour tout, je vous aime.

I would also like to extend a special thank you to my grandfather, a former English teacher who helped me to write this Tesis in English throughout the year.

RESUMO

As patologias do seio maxilar representam um desafio diagnóstico significativo devido à sua proximidade com estruturas dentárias e ósseas. Esta tese visa avaliar a contribuição do CBCT (Cone Beam Computed Tomography), uma técnica de imagem 3D mais avançada, no diagnóstico e no processamento terapêutico dessas patologias, em comparação com outras técnicas de imagem, como a radiografia panorâmica convencional 2D, a tomografia computadorizada (TC) e a ressonância magnética (RM). De fato, as varreduras CBCT são frequentemente utilizadas em odontologia para visualizar as estruturas orais e maxilofaciais, incluindo os dentes, ossos maxilares e o seio maxilar.

Primeiramente, analisaremos a anatomia e a fisiologia do seio maxilar, destacando as características estruturais que influenciam as decisões diagnósticas.

O seio maxilar está intimamente relacionado com as raízes dos dentes posteriores da maxila, havendo uma frequência de doenças mucosas e sinusites de origem dentária. Além disso, compreender a anatomia do seio maxilar e seus componentes neurovasculares é essencial tanto para cirurgias do seio quanto para complicações relacionadas a procedimentos cirúrgicos orais.

Em seguida, será realizada uma comparação das vantagens e desvantagens dos diferentes métodos de imagem, com resolução da imagem, precisão, exposição à radiação e custos associados.

As indicações clínicas do CBCT serão então discutidas, com foco em seu papel no planejamento cirúrgico, manejo de complicações, elevação do seio, extrações dentárias e acompanhamento pós-operatório. A avaliação pré-operatória do seio maxilar é essencial para o sucesso dessas cirurgias.

Desde sua introdução no final dos anos 1990, o CBCT tornou-se um método diagnóstico comum. No entanto, o uso do CBCT e a seleção do protocolo de captação de imagens devem ser baseados em boas práticas, considerando a qualidade da imagem e o nível de exposição à radiação do paciente.

É essencial estar ciente desses limites como medida de proteção radiológica para evitar a recorrência desnecessária desses exames.

Palavras-chave: Seio maxilar, CBCT, Sinusite, Radiografia panorâmica

ABSTRACT

Maxillary sinus pathologies present a significant diagnostic challenge due to their proximity to dental and osseous structures. This thesis aims at evaluating the contribution of CBCT (Cone Beam Computed Tomography) the more advanced 3D imaging modalities, in the diagnosis and therapeutic management of these pathologies, compared to other imaging techniques such as conventional panoramic radiography 2D or computed tomography (CT scans) computed tomography, and magnetic resonance imaging (MRI). Indeed, CBCT scans are often used in dentistry to visualize the oral and maxillofacial structures, including teeth, jawbones, and sinus maxillary.

First, we shall analyze the anatomy and physiology of the maxillary sinus, highlighting the structural features that influence diagnostic decisions.

The maxillary sinus is intimately related to the roots of the posterior maxillary teeth, there is a frequency of mucosal diseases and sinusitis of dental origin. Moreover, understanding the anatomy of the maxillary sinus and its neurovascular components is essential both for sinus surgeries and for complications related to oral surgical procedures.

Then, a comparison of the advantages and disadvantages of different imaging methods will be conducted, with a particular focus on image resolution, precision, radiation exposure, and associated costs.

The clinical indications of CBCT will then be discussed, with a focus on its role in surgical planning, complication management, sinus lift, dental extractions and post-operative follow-up. Pre-operative assessment of the maxillary sinus is essential for the success of this surgery.

Since its introduction in the late 1990s, CBCT has become a common diagnostic method. However, the use of CBCT and the selection of scanning protocol must be based on a good practice considering the required image quality and the patient's radiation exposure level.

It is essential to be aware of these limits as a radiation protection measure to prevent unnecessary recurrence of these examinations.

Key Words: Maxillary sinus, CBCT, Sinusitis, Panoramic X-ray

RESUMÉ

Les pathologies du sinus maxillaire posent un défi diagnostique en raison de leur proximité avec les structures dentaires et osseuses. Cette thèse vise à évaluer la contribution du CBCT (Cone Beam Computed Tomography) dans le diagnostic et la prise en charge de ces pathologies, par rapport à d'autres techniques d'imagerie telles que la radiographie panoramique, les scanners (tomodensitométrie) et l'IRM (imagerie par résonance magnétique). Les CBCT sont utilisés en dentisterie pour visualiser les structures orales et maxillo-faciales, les dents, les os de la mâchoire et les sinus maxillaires.

Nous analyserons l'anatomie et la physiologie du sinus maxillaire, en soulignant les caractéristiques structurelles qui influencent le diagnostic. Le sinus maxillaire est lié aux racines des dents maxillaires postérieures, il existe une fréquence de maladies muqueuses et des sinusites d'origine dentaire. De plus, la compréhension de l'anatomie du sinus maxillaire et de sa partie neurovasculaire est essentielle, tant pour les interventions chirurgicales du sinus que pour les complications liées aux procédures chirurgicales orales.

Ensuite, nous verrons les avantages et inconvénients des différentes méthodes d'imagerie, en mettant l'accent sur la résolution d'image, la précision, l'exposition aux radiations et les coûts associés.

Les indications cliniques du CBCT seront abordées, en se concentrant sur son rôle dans la planification chirurgicale, la gestion des complications, les élévations sinusiennes, les extractions dentaires et le suivi post-opératoire. L'évaluation préopératoire du sinus maxillaire est essentielle pour le succès de différentes chirurgies.

Depuis son introduction dans les années 1990, le CBCT est devenu une méthode de diagnostic courante. Cependant, l'utilisation du CBCT et le choix du protocole de numérisation doivent s'appuyer sur une bonne pratique en fonction de la qualité d'image et du niveau d'exposition aux radiations du patient.

Il est essentiel de connaître ces limites comme mesure de radioprotection afin de prévenir les répétitions inutiles de ces examens.

Mots-clés : Sinus maxillaire, CBCT, Sinusite, Radio panoramique

INDEX

FIGURES INDEX	9
TABLES INDEX	13
LIST OF ABBREVIATIONS	15
INTRODUCTION	17
I. Maxillary Sinus Anatomy and Physiology	19
I.1. Anatomy of the Maxillary Sinus	19
I.1.1. Morphology of the Maxillary Sinus	19
I.1.2. Vascularization of the Maxillary Sinus	22
I.1.3. Innervation of the Maxillary Sinus	24
I.2. Physiology of Maxillary Sinus	24
I.2.1. Pneumatization of the Maxillary Sinus	24
I.2.2. Histology of Maxillary Sinus	25
I.2.3. Function of the Maxillary Sinus	26
I.3. Particularities of the Maxillary Sinus	27
I.3.1. Proximity of dental roots	27
I.3.2. Anatomical variations	30
II. Different Imaging Techniques for the Maxillary Sinus	31
II.1. Principle of operation	31
II.1.1. CBCT	31
II.1.2. Panoramic radiography	34
II.1.3. Computed Tomography	37
II.1.4. Magnetic Resonance Imaging	38
II.1.5. Ultrasonography	40
II.2. The limits of the different imaging techniques	42
II.2.1. CBCT	42
II.2.2. Panoramic radiography	43
II.2.3. Computed tomography	44
II.2.4. MRI	46
II.2.5. Ultrasonography	47
II.3. Comparison of the difference techniques	48

II.3.1.	Resolution and Precision	48
II.3.2.	Radiation Exposure.....	50
II.3.3.	Artifacts and Limitations	51
II.3.4.	Costs and Accessibility	54
II.3.5.	Safety and radioprotection.....	55
III.	Role of the CBCT in Maxillary Sinus Pathologies.....	57
III.1.	Diagnosis of Maxillary Sinus Pathologies	57
III.1.1.	Maxillary sinusitis: Dental or non-dental origin.....	57
III.1.2.	Cysts and pseudocyst	59
III.1.3.	Malignant and benign tumors	61
III.1.4.	Maxillary Sinus fractures	63
III.1.5.	Oral-sinus communication.....	65
III.2.	CBCT-guided Therapeutic Choices.....	67
III.2.1.	Surgical planning	67
III.2.2.	Maxillary sinus floor augmentation (sinus lift)	68
III.2.3.	Trans-sinus implant.....	71
III.2.4.	Postoperative follow-up.....	72
CONCLUSION	75

FIGURES INDEX

Figure 1 : Lateral paranasal sinus dissection (from Atlas of human anatomy 7 th Edition Frank H. Netter).....	20
Figure 2 : Coronal section of the facial mass through the maxillary sinus. 1- Zygomatic Recess; 2- Palatine Recess; 3-Alveolar Recess; 4- Maxillary sinus ostium. Adapted from Delmas (2019)	21
Figure 3: Vasculature of the maxillary sinus and its surrounding structures (Mularczyk & Welch, 2024).....	22
Figure 4 : Schematic representation of the alveolar antral artery as anastomosis of the posterior superior alveolar artery with the infraorbital artery (Valente, 2016).....	23
Figure 5 : Histological section of a maxillary sinus mucosa. 40x magnification. Cc: Caliciform cells (Eloy et al., 2005).....	25
Figure 6 : Classification of the vertical relationships between the root apex of the maxillary tooth and the inferior wall of the maxillary sinus in the coronal section, adapted from (Oishi et al., 2020).....	28
Figure 7 : CBCT, Principle of basis image acquisition where in X-ray source and Image receptor reciprocate around patient 180 – 360 degrees to acquire 2D cephalometric images (Venkatesh & Venkatesh Elluru, 2017)	31
Figure 8: CBCT acquisition and display modes A – Acquired 2D Basis images; B – axial view ; C – coronal view; D – sagittal view; E- MPR view; F - Curved slices; G - Cross-sectional view; H - Ray sum comprising images of increased section thickness; I – Volumetric images of DVR; J- Volumetric images of IVR (Venkatesh & Venkatesh Elluru, 2017).....	32
Figure 9: A - Cylindric shape and measurement characteristics of the FOV; B - The different FOV options size from the CBCT (Venkatesh & Venkatesh Elluru, 2017).....	33
Figure 10: Panoramic radiography taken by the author	34
Figure 11: Producing a panoramic image according to Sanjay M. Mallya and Alan G. Lurie (https://pocketdentistry.com/10-panoramic-imaging/).....	35
Figure 12: The Focal Trough from Sanjay M. Mallya and Alan G. Lurie (https://pocketdentistry.com/10-panoramic-imaging/)	36
Figure 13: CT-scan of the sinuses. Coronal section of the complete filling of the left maxillary sinus and ipsilateral anterior ethmoidal cells (https://www.information-dentaire.fr/formations/chec-du-traitement-dune-sinusite-chronique-maxillaire/).....	38

Figure 14: Facial MRI, coronal section sequence T2: tissue thickening of 23 mm of major axis in relation to the left middle meatus with a heterogeneous T2 signal aspect (https://www.information-dentaire.fr/formations/chech-du-traitement-dune-sinusite-chronique-maxillaire/).....	40
Figure 15: Right maxillary sinus ultrasound (Blanco et al., 2015).....	41
Figure 16 : Synthetic panoramic images (right) along a curve drawn in the axial plane (left) (Pauwels et al., 2015)	43
Figure 17: The fan beam upon which spiral computed tomography is based interrogates only a slice of tissue, whereas the cone beam of cone-beam computed tomography interrogates a 3-dimensional region within a 360° rotation (MacDonald-Jankowski & Orpe, 2006).	45
Figure 18 : Artificial increase in image noise (Pauwels et al., 2015).....	50
Figure 19 : Axial view of mandible and cervical vertebra. Thick arrows: aliasing artefact (Olszewski, 2020).....	52
Figure 20: Axial view of mandible. Arrows: ring artifact visible in the middle of the mouth floor (Olszewski, 2020).....	52
Figure 21: Axial view of mandible and of cervical spine. Thick arrows: complex pattern of streaks due to crowns and bridge present on all upper teeth. Thin arrows: aliasing artifact (Olszewski, 2020)	53
Figure 22: Different types of CBCT gantries. Left: seated patient position (3D Accuitomo® 170; J. Morita, Kyoto, Japan). Right: standing patient (WhiteFox®; Acteon Group, Merignac, France).....	54
Figure 23: A straight burr impinged into the left maxillary sinus (Tilaveridis et al., 2022).....	55
Figure 24: Multiplication of bacteria invading from the focus of a dental infection results in odontogenic (Sumathy & Muthiah, 2020).	57
Figure 25: CT scan, axial section: incomplete opacity of the lower left maxillary sinus with foreign body image (Gilain & Laurent, 2005).....	58
Figure 26: Odontogenic sinusitis with opacification of the right maxillary sinus as a result of a dental infection (coronary, sagittal, axial views) (Langlais et al., 2009).....	59
Figure 27: CBCT image of a patient with a mucous retention cyst that was diagnosed at the lateral wall of the right maxillary sinus (Yeung et al., 2018)	60
Figure 28: Cone-beam computed tomography (CBCT) scans of the radicular cyst in the maxillary sinus. A- The coronal view clearly shows the right maxillary sinus filled	

with cyst in the proximity to the infraorbital canal and the floor of the orbit; B - The axial view clearly shows the cystic lesion in the maxillary sinus, with thinning and perforation of the cortical plate on the medial aspect of the maxilla; C- The sagittal view of the maxilla shows the expansive lesion with posterior growth in the maxillary tuber (Biocanin, 2015) 61

Figure 29 : Sinusal carcinoma seen at the CBCT. A - Proliferative growth seen on the alveolar mucosa of left side of maxilla; B - Coronal section of the CBCT; C - Sagittal section of the CBCT (left side); D - Axial section of the CBCT. (Ali et al., 2015)..... 62

Figure 30: View from the Coronal plane. The CBCT shows a fracture line along the floor of the maxillary sinuses (Ahmed et al., 2023). 64

Figure 31: The Caldwell - Luc procedure. A - If a root or foreign body enters the sinus, the socket is widened buccally after lifting a mucoperiosteal flap ; B - A small opening is made in the bone, 1 cm above the first premolar apices ; C - Saline is injected into the sinus, then suction is applied via the socket or the opening (Sumathy & Muthiah, 2020). 65

Figure 32 : Multiplanar reformatted cone-beam computed tomographic images of a oral-sinus communication. A- Axial view shows loss of the buccal cortical plate in the right maxillary first molar extraction site and loss of both buccal and lingual cortical plates in the left maxillary first molar extraction site ; B - Sagittal view shows loss of cortication in the left maxillary sinus ; C - Coronal View shows the extraction sockets ; D - A volume-rendered image shows the loss of the cortical plate at the left maxillary first molar's extraction site (Shahrou et al., 2021). 66

Figure 33: Lateral window approach for sinus augmentation (George et al., 2020)..... 69

Figure 34: A crestal approach for sinus floor elevation (George et al., 2020)..... 69

Figure 35 : Illustration of trans-sinus implant placement (left) compared tozygomatic implant placement (right) and the associated anatomy (Aalam et al., 2023) 71

TABLES INDEX

Table 1: Average bone thickness between the apices of the roots and the maxillary sinus (Kang S, 2015)	29
Table 2 : The multi FOV selection according to Vatech® Vatech America, 2025, adapted from Green X – Features (https://www.vatechamerica.com/products/green-x#!features).....	33
Table 3: Absolute and relative contraindications to MRI (Conroy et al., 2021).....	47
Table 4: Comparaison of radiation dose from different techniques from the Federal Nuclear Control Agency (https://afcn.fgov.be/fr/dossiers/applications-medicales/comparaison-des-doses-de-rayonnements).....	51

LIST OF ABBREVIATIONS

ALADA - As Low As Diagnostically Acceptable

ALARA - As Low As Reasonably Achievable

ALADAIP - As Low As Diagnostically Acceptable being Indication-oriented and Patient-specific

CBCT - Cone Beam Computed Tomography

CCD - Charge-Couple Device

CMOS - Complementary Metal Oxide Semiconductor

CT - Computed Tomography

CT-SCAN - Computerized Tomography Scanner

DICOM - Digital Imaging and Communication in Medicine

FOV - Field of View

OAC - Oro-antral communication

OAF - Oro-antral fistula

IOA - Infra orbital artery

MA - Maxillary Artery

MRI - Magnetic Resonance Imagery

OPG - Orthopantomography

ORL - Otorhinolaryngologist

PSAA - Posterior superior alveolar artery

3D - Three dimensional

INTRODUCTION

In the human body, there are four pairs of paranasal sinuses. The maxillary sinus is undoubtedly the largest and biggest of all the sinuses. There are also the ethmoid sinuses, the frontal sinuses, and the sphenoid sinuses. These air-filled cavities are pyramid-shaped and located above the posterior dentoalveolar region of the maxilla and communicate directly with the tracheobronchial tree and lungs (Whyte & Boeddinghaus, 2019).

The maxillary sinus was first described and illustrated by Leonardo Da Vinci in 1489, but the first precise anatomical description was made in 1651 by Nathanael Highmore, thus the alternative term for the maxillary sinus being « Antrum of Highmore ». Highmore was one of the first to describe the relationship between the maxillary sinuses and the teeth with his various anatomical plates, but it took more than a century for this work to be recognized and for sinus pathologies to be considered and begin to be treated (Jankowski et al., 2016).

Today these anatomical structures are important to respiratory and dental health. Several complications can occur in these sinuses, including sinusitis, cysts, pseudocysts, tumors, intrusion of foreign bodies, osseous and dental pathologies, or even anatomic variations, which may lead to certain challenges (Ahmed et al., 2023).

The management and treatment of these pathologies require advanced imaging techniques. For many decades, diagnostic imaging primarily relied on two-dimensional (2D) radiography. The advent of three-dimensional (3D) imaging marked a major step forward, leading to the development of cone-beam computed tomography (CBCT), which was introduced in the early 1990s independently by Arai (1992) in Japan and Mozzo (1995) in Italy (Kiljunen et al., 2015). Cone-beam computed tomography, first emerged with its initial device, the NewTom 9000, in 1996, developed by a company called Quantitative Radiology based in Verona, Italy. Preliminary results were published in 1998 by Mozzo and colleagues, although a CBCT device specific to dentistry had already been introduced in 1995 (De Marneffe et al., 2017).

CBCT has become increasingly indispensable in clinical practice for implant planning, sinus augmentation, orthodontics, and endodontics in the detection of complex pathologies in dental roots. It is also valuable for diagnosing conditions such as periapical lesions, periodontal diseases, trauma, internal and external resorptions, mucous retention cysts, and anatomical variations like sinus septa or sinus hypoplasia (Yeung et al., 2022).

The integration of CBCT into diagnostics is now essential in dental and sinus treatments. As these procedures become more sophisticated, the risks and complications, often linked to the maxillary sinuses, also increase. Thus, accurate imaging has become paramount for both diagnosis and therapeutic planning.

This thesis aims to highlight the essential role of CBCT in diagnosing and managing maxillary sinus pathologies. By exploring its advantages, such as anatomical accuracy and volumetric visualization, CBCT proves invaluable. However, as with all ionizing devices, CBCT is governed by radioprotection principles and best practice recommendations.

I. Maxillary Sinus Anatomy and Physiology

I.1. Anatomy of the Maxillary Sinus

I.1.1. Morphology of the Maxillary Sinus

The maxillary sinuses are air cavities that can be symmetrical or asymmetrical and develop in the maxillary bone. It is a bone belonging to the viscerocranium and of membranous origin that develops from an evagination of the nasal mucosa (Gaudy & Gorce, 2011). They have three recesses: the alveolar process, zygomatic recess, and infraorbital recess, and drain into the middle meatus of the nasal cavity (Yeung et al., 2022). From birth, the sinus grows as an invagination into the maxilla, being the first sinus to develop. This growth increases with the first dentition, between 0 and 3 years of age, then between 7 and 12 years of age, and more gradually until the appearance of the upper third molars at around 17 years of age (Klossek et al., 2007).

In terms of dimensions, the size of the maxillary sinus at the adult age is almost identical for men and women, with no significant differences in size between individuals with or without sinus pathologies. However, there are differences in sinus floor height and volume (Möhlhenrich, 2015). The average dimensions of the maxillary sinus for an individual are 45 mm x 25 mm x 38 mm (anteroposterior/depth x lateral/width x vertical/height), for an average total volume of 141 mm³ (Sayáns et al., 2020).

Lateral dissection

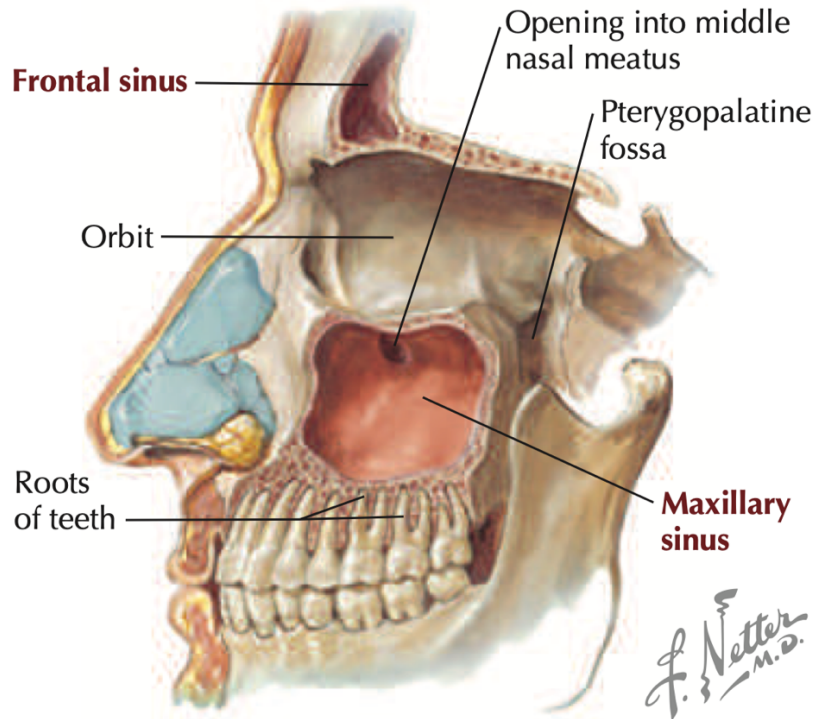


Figure 1 : Lateral paranasal sinus dissection (from Atlas of human anatomy 7th Edition Frank H. Netter)

The maxillary sinus (Figure 1) is a pyramidal cavity with a medial base corresponding to the lateral wall of the nasal cavity and a lateral apex extending into the zygomatic process of the maxilla (Kamina, 2009).

It presents five walls and five recesses. The five walls are the following (Kamina, 2009) :

- The superior wall corresponds to the orbital floor
- The inferior wall is formed by the alveolar process of the maxilla and is related to the apex of the roots of the maxillary premolars and molars, which may explain the perception of protrusions in this sinus.
- The posterior or posterolateral wall is in contact with the infratemporal and pterygopalatine fossae.
- The medial wall includes the base of the lateral wall of the nasal cavities and the ethmoid in its upper part.
- The anterolateral wall, forming the apex of the sinus, extends into the zygomatic process up to the infraorbital foramen.

The five recesses (Figure 2) are the following (Delmas, 2018):

- The zygomatic recess, which emerges at the body of the zygoma.
- The palatine recess, which is in the hard palate.
- The alveolar recess, which expands into the alveolar process of the maxilla.
- The orbital recess, which extends into the maxilla up to the inner edge of the orbit.
- The tuberosity recess, which can be observed near the upper third molar.

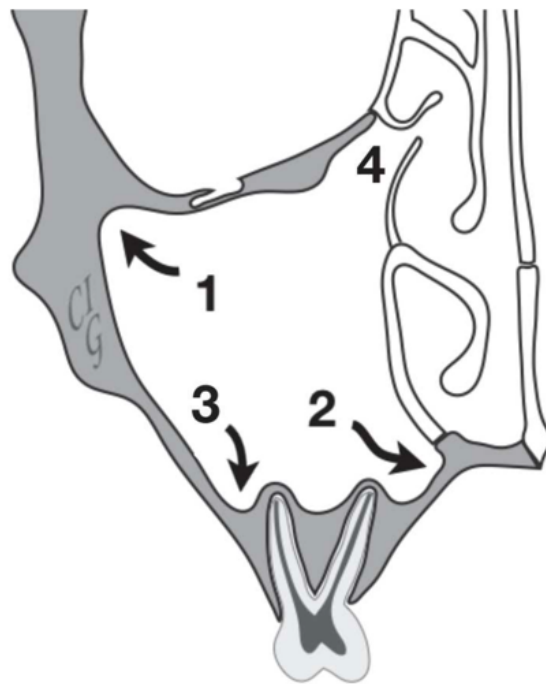


Figure 2 : Coronal section of the facial mass through the maxillary sinus. 1- Zygomatic Recess; 2- Palatine Recess; 3-Alveolar Recess; 4- Maxillary sinus ostium. Adapted from Delmas (2019)

The alveolar process of the maxilla, which is well known in dentistry, forms the bony support for the teeth and constitutes its inferior floor. It is a truncated pyramid with an internal base (Vacher, 2013).

Finally, there is a communication with the nasal cavities at the level of the medial wall of the maxillary sinus, also known as the maxillary sinus ostium (Delmas, 2018).

I.1.2. Vascularization of the Maxillary Sinus

The vascularization of the maxillary sinus (Figure 3) depends on the maxillary artery (MA), which is one of the terminal branches of the external carotid artery. Passing through the pterygopalatine fossa, it produces the following 3 collateral branches (Iwanaga et al., 2019):

- The infraorbital artery (IOA) passes below the orbit at the floor level, exiting the infraorbital canal and foramen to vascularize the lower sinus wall, the anterior teeth, incisors and canines via the anterosuperior alveolar arteries and even the cheek.
- The posterior superior alveolar artery (PSAA) located on the medial wall of the sinus, vascularizes the posterior teeth, maxillary molars and premolars and the gingiva.
- The posterior lateral nasal artery arises from the sphenopalatine artery and can be found from the level of the medial wall to the posterior wall.

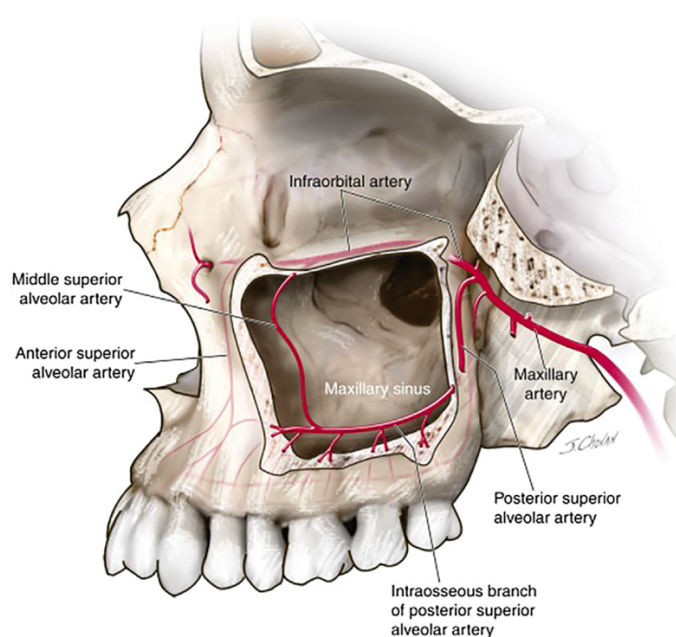


Figure 3: Vasculature of the maxillary sinus and its surrounding structures (Mularczyk & Welch, 2024)

The greater palatine artery also plays a role in the vascularization of the maxillary sinus, irrigating the lower wall of the maxillary sinus via its multiple branches on the hard palate (Vacher, 2013).

The anastomosis of the PSAA and IOA, at the level of the lateral wall, forms the antral alveolar artery to irrigate the lateral wall of the sinus, the mucosa and the membrane of the maxillary sinus (Schneider's membrane), which will be described later (Mularczyk & Welch, 2024).

The antral alveolar artery (Figure 4) can lead to significant bleeding complications in certain procedures, such as sinus augmentation procedures; therefore its preoperative detection using CBCT is crucial (Valente, 2016).

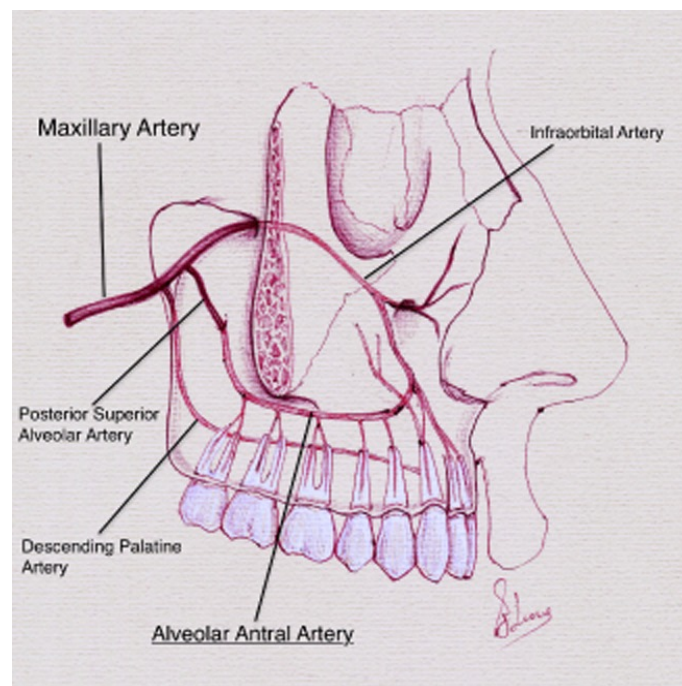


Figure 4 : Schematic representation of the alveolar antral artery as anastomosis of the posterior superior alveolar artery with the infraorbital artery (Valente, 2016)

Venous drainage is carried out through the pterygoid venous plexuses and the parotid venous plexus, posteriorly through the maxillary vein, and anteriorly through the facial vein and then to the internal jugular vein (Delmas, 2018).

The lateral wall of the maxillary sinus at the level of the nasal cavities, on the other hand, will be drained by the sphenopalatine vein (Whyte & Boeddinghaus, 2019).

Lymphatic drainage is carried out by collectors at the level of the middle meatus to reach the preauricular lymphatic plexus and then to the cervical lymph nodes (Pommer, 2012).

I.1.3. Innervation of the Maxillary Sinus

The innervation of the maxillary sinus is made possible by the trigeminal nerve, the 5th cranial nerve, and in particular through its second branch, the maxillary nerve (V2).

The V2 nerve will give the infraorbital nerve, which is purely sensitive. Through the infraorbital canal it will give anterior and superior branches which innervate the entire dental plexus and the anterior and superior part of the maxillary sinus (Norton, 2011).

The infraorbital nerve will also give the middle and anterior branches of the alveolar nerve before emerging from the infraorbital foramen which will innervate this time the intraosseous wall of the sinus and anterior as well as the entire alveolar process to innervate the maxillary teeth (Pommer, 2012).

The maxillary part of the trigeminal nerve, passing through the pterygopalatine fossa and entering the infratemporal fissure, will give rise to the posterior and superior branch of the alveolar nerve. It crosses the posterolateral sinus wall, travels between the bone and the sinus membrane in an extraosseous position to innervate the posterior and middle part of the sinus. (Whyte & Boeddinghaus, 2019) (Iwanaga et al., 2019)

I.2. Physiology of Maxillary Sinus

I.2.1. Pneumatization of the Maxillary Sinus

Maxillary sinus pneumatization is the physiological process that allows the development and enlargement of the maxillary sinus. (Göksel & Güler, 2023)

It is performed from the infant in the form of an invagination that sinks into the maxilla and develops fully with the appearance of the first maxillary decidual teeth to reach the various anatomical landmarks and especially to reach the floor of the nasal cavities at about 17 years of age, when the maxillary growth is complete (Klossek et al., 2007).

This pneumatization continues during adulthood and can be marked by periods of interruption or stagnation, particularly following tooth loss and especially following edentulism in the posterior, premolar and molar teeth (Elsayed et al., 2023).

In some cases, this can lead to a union of the sinus floor and the alveolar ridge, which can lead to an even greater increase in the volume of the maxillary sinus. In some severe cases, only a small thin bone plate separates the lower jaw from the oral cavity (Pommer, 2012).

Indeed, the bone resorption induced by the loss of posterior teeth in this maxillary region promotes the descent of the sinus floor, making the bone height insufficient for the placement of implants, for example (Elsayed et al., 2023).

It is also shown that pneumatization varies between individuals and can be influenced by factors other than edentulism such as infections, previous periodontal disease, facial trauma or even simply the quality or quantity of the alveolar bone (Elsayed et al., 2023).

I.2.2. Histology of Maxillary Sinus

The walls of the maxillary sinus as well as the nose and all the air cavities of the face are covered by a mucous membrane of the respiratory type. Formerly called Schneider's membrane in homage to the Anatomy Professor, this mucous membrane is made up of two layers, a thin and deep one that allows the cilia to move easily and another more superficial one that can be able to capture the inhaled particles. This mucosa includes a respiratory-type epithelium, a chorion, and a basement membrane, as seen in figure 5 (Whyte & Boeddinghaus, 2019).

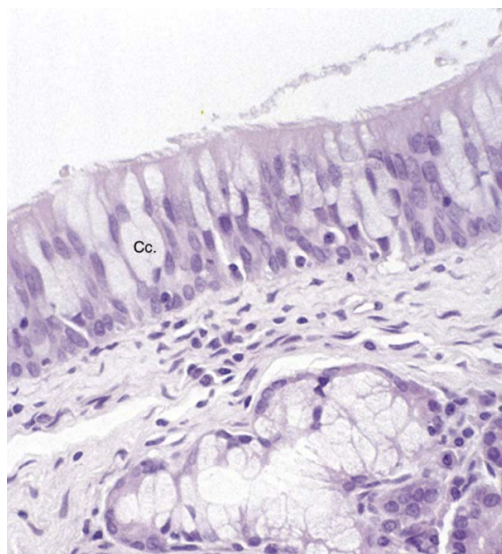


Figure 5 : Histological section of a maxillary sinus mucosa. 40x magnification. Cc: Caliciform cells (Eloy et al., 2005)

The pseudostratified respiratory epithelium, of the ciliated cylindrical type, is made up of 4 cell types (Eloy et al., 2005) :

- Basal cells which ensure cell renewal.
- Caliciform cells (Figure 5), which synthesize the necessary mucins and contribute to the composition of mucus.
- Microvilli cells that allow fluid exchange and the maintenance of the periciliary aqueous film.
- Ciliated cells, which represent 80% of the cell population, transport mucus to the ostium.

The chorion or lamina propria is a connective tissue composed of glands, nerves and vessels (less than in the nasal mucosa) in relation to the periosteum (Eloy et al., 2005). It includes 3 layers:

- A subepithelial layer rich immune cells
- A glandular layer that contains the various sero-mucosal and tubule-acinar glands.
- A vascular layer that is composed of a fenestrated capillary network.

The basement membrane is located just below the epithelium and above the chorion and is a thin junction layer allowing exchanges between the epithelium and the chorion (Eloy et al., 2005).

I.2.3. Function of the Maxillary Sinus

The exact role of the maxillary sinuses is not exactly known, but they play important roles. In particular, they play a key role in mucociliary clearance or drainage, the filtration and protection mechanism essential to the respiratory tract. This process allows the action of the cilia and the mucus layer to capture particles, bacteria, viruses and other irritants in order to protect the underlying epithelium and the respiratory tract by preventing bacterial proliferation and in evacuating foreign particles via the ostium of the middle meatus and towards the nasal cavities (Eloy et al., 2005).

In addition to this protective role, the sinuses participate in the humidification and warming of the inhaled air before it reaches the lungs as well as in terms of gas exchange in the regulation of local pressure. Indeed, the exchanges between oxygen (O₂) and

carbon dioxide (CO₂) take place at this level, and any alteration of this partial pressure equilibrium in O₂ or CO₂ can result in a slowing down of mucociliary clearance (Eloy et al., 2005).

Secondly, the maxillary sinuses also have more structural roles because being air cavities, they participate in the lightening of the skull and absorb shocks in the event of facial trauma while maintaining the rigidity necessary for mastication or minor traumas.

Finally, thanks to their airy architecture, they make it possible to modulate the voice and play a kind of modulation of the timbre of the voice thanks to the sinus cavities which act the role of resonance boxes (Whyte & Boeddinghaus, 2019).

I.3. Particularities of the Maxillary Sinus

I.3.1. Proximity of dental roots

The anatomical proximity between the roots of the posterior maxillary teeth and in particular the molars and the floor of the maxillary sinus makes the latter susceptible to dental infections (Jung & Cho, 2012).

The thinness of the bone separating the roots of the posterior maxillary teeth from the maxillary sinus can fracture during tooth extractions, potentially causing a communication between the oral cavity and the maxillary sinus, which is called an iatrogenic oral-antral communication (Regnstrand et al., 2021).

This proximity increases the risk of spreading odontogenic infections to the maxillary sinus that can lead to dentary-induced maxillary sinusitis (Premoli Maciel et al., 2020).

There is a classification of the position of the apexes (Figure 6) and periapical lesions in relation to the sinus floor into three classes (Oishi et al., 2020):

- Apex Classe I: Distinct distance between the root tip and sinus floor
- Apex Classe II: The root tip touches the sinus floor
- Apex Classe III: The root tip overlaps the sinus floor

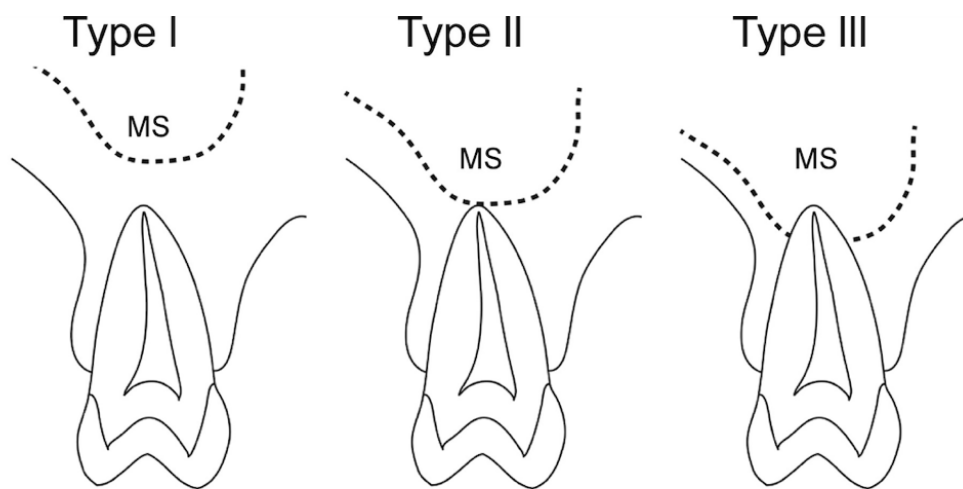


Figure 6 : Classification of the vertical relationships between the root apex of the maxillary tooth and the inferior wall of the maxillary sinus in the coronal section, adapted from (Oishi et al., 2020)

This proximity is assessed using periapical radiographies and it is therefore difficult to determine radiographically using this type of conventional radiograph whether there is a perforation of the maxillary sinus. However, when a radiography shows us a class I apex, there is an 82.5% chance that an oral-antral communication does not exist (Oberli et al., 2007) The chances of a complication occurring are then 2.77 times higher when the tooth root is in direct contact with the maxillary sinus (Premoli Maciel et al., 2020).

The prevalence of proximity between the maxillary sinus and the teeth between men and women is not significative, but after the loss of a tooth the sinus and membrane will pneumatize in the coronal direction and the direction of the bony crest in the apical direction (Kang et al., 2015).

The roots of the second premolar and the first two maxillary molars are frequently closely related to the maxillary sinus (Table 1), wisdom teeth and first premolars because they are related only if the maxillary sinus occupies a very large volume (Kang et al., 2015).

Table 1: Average bone thickness between the apices of the roots and the maxillary sinus (Kang S, 2015)

Maxillary tooth roots	Distance between apices and bone
First premolar vestibular root	1,05 mm
First Premolar palatine root	5,16 mm
Second Premolar vestibular root	2,46 mm
Second Premolar palatine root	5,98 mm
First molar mesio-vestibular root	3,00 mm
First molar disto-vestibular root	3,13 mm
First molar palatal root	12,16 mm
Second molar mesio-vestibular root	4,99 mm
Second molar disto-vestibular root	3,99 mm
Second molar palatal root	10,62 mm

About 40% of maxillary sinusitis cases are associated with the teeth, as various odontogenic factors can initiate or maintain inflammatory and infectious processes of the maxillary sinus such as cavities, periodontal diseases and odontogenic cysts

The symptoms are different but, in the majority, can be associated to pain, headaches, facial tenderness, congestion and nasal secretion (Premoli Maciel et al., 2020).

A periapical lesion close to the maxillary sinus can increase the risk of sinus disease, as bacteria and toxins present in apical lesions can infiltrate due to the contiguity of the root apex and sinus floor into the maxillary sinus by diffusion through the porous maxillary bone or via blood vessels resulting in thickening of the sinus mucosa (Premoli Maciel et al., 2020)

The thickness of the Schneider membrane for healthy individuals is between 1.18 mm and 1.21 mm. The usual cutoff to differentiate a normal membrane from a thickened membrane is 2 mm (Yeung et al., 2022).

The prevalence of a thickened membrane depends on age and sex, but especially on the presence of periodontal lesions, class II or III furca lesions and vertical bone loss greatly increasing the thickening of the membrane and therefore the cause of odontogenic maxillary sinusitis (Huang et al., 2021).

I.3.2. Anatomical variations

The maxillary sinus is characterized by significant anatomical variations. These variations can have clinical consequences and can lead to certain risks or complications during surgical procedures. The most important variation is the presence of the maxillary septa. These cortical bone walls, which vary in number, thickness and length, can divide the sinus into two or more cavities. The probable origin of these septa are the lower and lateral walls of the sinus for septa of dental origin, their development is linked to the different phases of dental eruption. A separation inside the maxillary sinus may also be observed (Iwanaga et al., 2019).

Finally, the maxillary sinus may present accessory ostia. Generally single, but sometimes multiple, these additional openings can be congenital or following sinus pathologies. Obstruction of the main ostium, maxillary sinusitis or different anatomical and pathological factors in the middle meatus are possible mechanisms involved in their development (Maia Nobre Rocha de Miranda et al., 2011).

II. Different Imaging Techniques for the Maxillary Sinus

II.1.Principle of operation

II.1.1. CBCT

The Cone Beam Computed Tomography (CBCT) is a three-dimensional (3D) imaging method. It is a technique that is between panoramic radiography and conventional computed tomography (CT). But unlike CT, it uses a conical or pyramidal X-ray beam and a flat detector with reciprocal semi-conductors that rotates around the patient from 180 to 360 degrees (Jacobs & Quirynen, 2014).

This unique rotation captures many 2D projection images (Figure 7), similar to lateral cephalometric images that are then reconstructed using software into a 3D volumetric dataset. The number of these images may vary. The data is saved in DICOM format (Digital Imaging and Communication in Medicine) format (Venkatesh & Venkatesh Elluru, 2017).



Figure 7 : CBCT, Principle of basis image acquisition where in X-ray source and Image receptor reciprocate around patient 180 – 360 degrees to acquire 2D cephalometric images (Venkatesh & Venkatesh Elluru, 2017)

Like any X-ray machine, CBCT requires the production of X-rays, the attenuation of X-rays by an object, the detection of the signal, the processing of the image and the display of the images. In most units, the X-ray emission is pulsed at intervals during rotation to the next acquisition position. At each degree of rotation, the transmitter emits a pulse of X-ray that passes through the area of the human body and is received at the receiver (Abramovitch & Rice, 2014).

The image obtained by CBCT is a three-dimensional (3D) representation of the scanned region (Figure 7). It is an image consisting of three-dimensional pixels called voxels (volumetric pixels), and usually the associated software allows the data to be visualized in the form of multiplanar reconstructions (MPRs) displaying axial, sagittal and coronal sections.

In addition to these orthogonal views, secondary reconstructions can be generated such as oblique sections, curved sections simulating a panoramic view, cross-sections and also depending on the software an associated 3D reconstruction.

Visualization can also be done by direct volume rendering (DVR) and indirect volume rendering (IVR), including maximum intensity projection (MIP)(Figure 8). The images are characterized by a high spatial resolution, allowing to distinguish fine anatomical details such as impacted teeth, temporomandibular joint, calcifications, etc. The final images are normally free of distortion or magnification and the gray depth usually varies between 8 and 16 bits (Estrela et al., 2008; Venkatesh & Venkatesh Elluru, 2017).

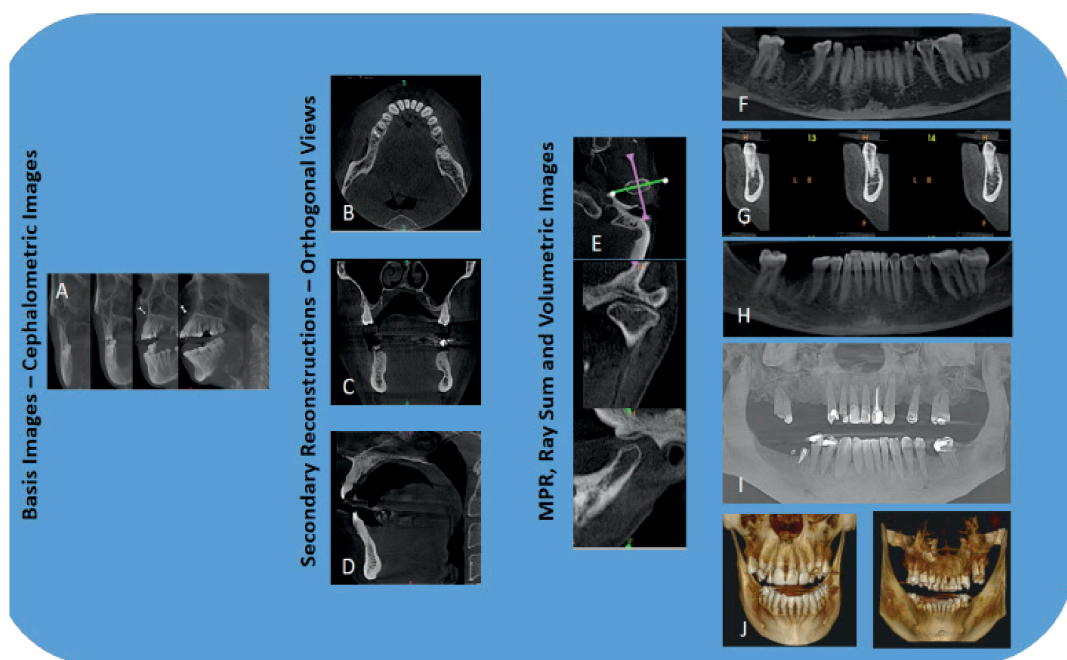


Figure 8: CBCT acquisition and display modes A – Acquired 2D Basis images; B – axial view ; C – coronal view; D – sagittal view; E- MPR view; F - Curved slices; G - Cross-sectional view; H - Ray sum comprising images of increased section thickness; I – Volumetric images of DVR; J- Volumetric images of IVR (Venkatesh & Venkatesh Elluru, 2017)

The field of view (FOV) represents the volume of the patient's anatomy that is imaged at the time of acquisition, usually cylindrical or spherical in shape and is defined by its height (H) and the diameter of its base (D) (Figure 9). Many CBCT units now have the

capability of scanning a range of FOV sizes. Today, the choice to use different sizes of FOV is fundamental for several reasons (Abramovitch & Rice, 2014).

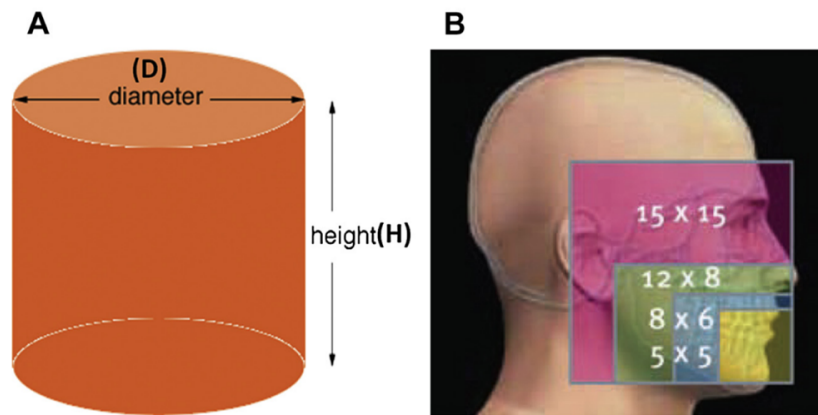


Figure 9: A - Cylindric shape and measurement characteristics of the FOV; B - The different FOV options size from the CBCT (Venkatesh & Venkatesh Elluru, 2017).

First, in order to adapt and correspond to the anatomical area of interest for the diagnosis, a small FOV can be useful to visualize a few teeth, or just an evaluation of a periapical area (Table 2). Conversely, a larger FOV will be needed to observe the maxilla and mandible or even a larger one for more extensive craniofacial evaluations (Kiljunen et al., 2015).

Table 2 : The multi FOV selection according to Vatech® Vatech America, 2025, adapted from Green X – Features (<https://www.vatechamerica.com/products/green-x#!features>)

FOV 5X5	50mm/50mm	Single tooth capture	Implant single site Endo Perio 3 rd molar impactation
FOV 8x6	80mm/60mm	Single arch	Implantology Guided surgery Orthodontics
FOV 12x8	120mm/80mm	Dual arch	Surgical guides Sinus lift Bone grafting Bi lateral augmentation sinus
FOV 15x15	150mm/150mm	Sinus & TMJ	Surgical Guides Sinus lift for both sinus Complex orthognathic cases Simultaneous diagnosis for both TMJs

Secondly, the size of the FOV has an impact on the radiation dose received by the patient, in general a larger FOV exposes the patient to a higher radiation dose. The size should therefore be limited to the diagnostic area that is to be observed (Distefano et al., 2023).

Finally, FOV can indirectly influence image quality, a higher FOV can lead to an increase in diffuse radiation reaching the detector, which can increase noise and artifacts. Conversely, a FOV that is too small can lead to truncation artifacts. (Pauwels et al., 2015) In addition, to visualize fine details with high spatial resolution (potentially requiring small voxels), a smaller FOV, focused on the area of interest, is often preferred (Hosein Kiarudi et al., 2015).

II.1.2. Panoramic radiography

Panoramic radiography, also known as orthopantomography (OPG), is a two-dimensional dental imaging technique that provides a view of the upper and lower dental arches, the maxilla and the mandible (Figure 10). It was introduced by Paatero in the 1950s and made its clinical debut in the 1960s (Hallikainen, 1996).

It relies on the rotating movement of the X-ray source and the detector around the patient, generating a narrow beam that scans all the jaws. It does not take a static image like a periapical radiography for example. In this technique, the X-ray source and the receptor is located outside the patient's mouth (MacDonald & Telyakova, 2024).



Figure 10: Panoramic radiography taken by the author

The device rotates around the patient's head, involving a coordinated movement of the X-ray source and receiver around the patient to better fit the shape of the dental arch (Figure 11). This movement allows a certain layer of the jaws to be focused, where these structures appear sharp, while those structures outside of this focal layer appear blurred (Rushton & Horner, 1996).

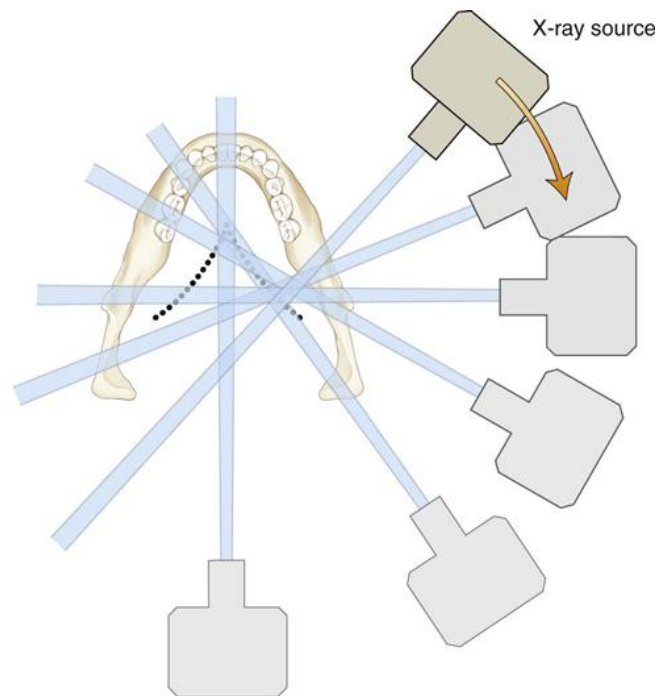


Figure 11: Producing a panoramic image according to Sanjay M. Mallya and Alan G. Lurie (<https://pocketdentistry.com/10-panoramic-imaging/>)

This movement creates a three-dimensional curved focus, called a "focal through" (Figure 12) which is designed to fit the shape of the dental arch. In fact, only the structures located inside this zone of netage are represented with an acceptable resolution, while the structures outside this zone appear blurred and invisible (Suparno et al., 2023).

OPG's technology has now evolved to better reflect the catenary shape of the dental arch, transitioning from a single center of rotation, to two, then three and finally, a continuously moving center (MacDonald & Telyakova, 2024).

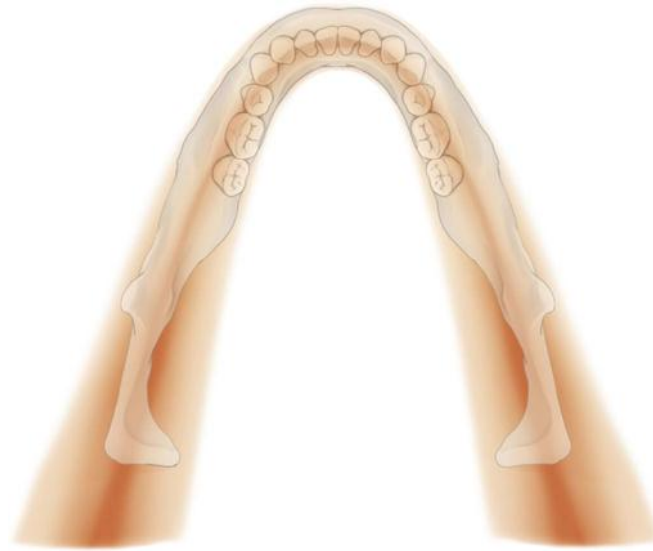


Figure 12: The Focal Trough from Sanjay M. Mallya and Alan G. Lurie (<https://pocketdentistry.com/10-panoramic-imaging/>)

Initially, OPG used silver film in combination with intensifying screens to capture the images, this analog process involved the chemical development of the film to visualize the latent image. The evolution towards digital accelerated in the 90s with the introduction of photo-stimulable phosphor plates (PSP) and solid-state detectors such as Charge-Couple Devices (CCD) and Complementary Metal Oxide Semiconductors (CMOS) (MacDonald & Telyakova, 2024).

Today, panoramic X-rays are mainly taken using a CCD/CMOS system. This technique now dominates the market (MacDonald & Telyakova, 2024).

- Concerning the CCD system:

The image is captured by a rigid sensor containing a thin silicon chip covered with a scintillator. When the residual X-ray beam hits the scintillator, The scintillator screen fluoresces when exposed to x-rays and forms a visible light radiographic image. It therefore emits visible light that releases electrons into the silicon chip, creating a potential difference. This analog information is then converted into digital values (pixels) by software. The resulting digital image can be displayed almost immediately on a computer monitor, allowing it to be analyzed. (White & Pharoah, 2008)

- Concerning the CMOS system:

The scintillator screen fluoresces when exposed to x-rays and forms a visible light radiographic image. The fiberoptic face plate couples the scintillator screen to the CMOS chip to reduce image noise. The CMOS imaging chip captures the light from the scintillator and creates a charge in each pixel proportional to the exposure. Each pixel is isolated from its neighbors and directly connected to a transistor. The sensor electronics read the charge in each pixel and transmits it to a computer. CMOS technology is cheaper, but it can have more noise in the image and a smaller acquisition area (Lacević & Vranić, 2004)

II.1.3. Computed Tomography

The computed tomography scan, or CT scan, is an advanced imaging modality that uses X-rays to produce three-dimensional images, usually displayed as sections. CT technology has been used for many years in dentistry to provide cross-sectional images for implant evaluation and studies of various infections, cysts, tumors, and trauma in the maxillofacial region (White & Pharoah, 2008).

Unlike CBCT, where the X-ray source makes a single rotation or less by emitting a cone beam into the region of interest, in CT imaging, the X-ray source moves helically around the patient many times, emitting a narrow-fan beam until the region of interest is covered. The patient's outgoing beam is captured by a digital sensor and a volume is then reconstructed to be viewed in any arbitrary plane (White & Pharoah, 2008).

CT offers soft tissue viewing windows that allow for the differentiation of various soft tissue densities (Figure 13). The use of intravenous contrast agents can further improve the contrast of soft tissues with greater vascularization, such as tumors. Thus, CT is particularly useful in situations where soft tissue details are important, such as determining whether a bone tumor has penetrated the bone cortex and has spread to adjacent soft tissues (White & Pharoah, 2008).



Figure 13: CT-scan of the sinuses. Coronal section of the complete filling of the left maxillary sinus and ipsilateral anterior ethmoidal cells (<https://www.information-dentaire.fr/formations/chech-du-traitement-dune-sinusite-chronique-maxillaire/>)

The CT can be used to evaluate potential implant sites in terms of the quantity and quality of remaining alveolar bone. An advanced application of CT is its fusion with positron emission tomography (PET) for the detection of abnormally elevated cellular metabolic rates, as observed in tumors (including metastases) and inflammatory diseases. Fused PET/CT imaging facilitates the precise anatomical localization of abnormal metabolic activity and has been shown to be useful in staging and treatment planning for squamous cell carcinoma or the adenoma carcinoma, which can affect the maxillary sinus (White & Pharoah, 2008).

II.1.4. Magnetic Resonance Imaging

Magnetic resonance imaging (MRI) is imaging technique that uses strong magnetic fields and radiofrequency waves to obtain high-quality images of soft tissues without the use of ionizing radiation (Kiran Kumar et al., 2021).

The principle of MRI is based on the alignment of the nuclei of hydrogen atoms present in the body with the magnetic field, followed by the emission of radio waves that cause

these nuclei to resonate. When these waves are interrupted, the nuclei release energy that is detected and used to create images (White & Pharoah, 2008).

The MRI is particularly useful for assessing soft tissues, such as the temporomandibular joints (TMJ), tongue, cheeks, salivary glands, and neck, as well as for detecting lymph node invasion or tumor spread along nerves (White & Pharoah, 2008).

Concerning the maxillary sinus, MRI is more specific than CT to characterize unilateral opacifications, making it possible to better differentiate neoplastic causes from infectious or inflammatory causes. MRI can delineate tumors from secretions and identify invasion of adjacent structures, including the skull base and orbit (Chua et al., 2021).

Magnetic resonance imaging (MRI) uses different sequences by manipulating radiofrequency pulses and magnetic gradients to visualize various tissues and pathologies (Chua et al., 2021):

- T1 weighted sequences (T1W): Sensitive to the longitudinal relaxation time of tissues, they are often used to visualize anatomy and fat, which appears shiny.
- T2 weighted sequences (T2W): Sensitive to transverse relaxation time and are particularly useful for detecting fluids, which appear with a high (bright) signal (Figure 14)
- Short Tau Inversion Recovery sequences (STIR): Sensitive to fluids, but with fat signal suppression, allowing for better visualization of edema or inflammation
- Contrast Medium Sequences (Gadolinium): Following administration of gadolinium, T1 sequences weighted with fat saturation are often used to assess tissue enhancement. This enhancement may indicate increased vascularization associated with inflammatory or tumor processes.
- Diffusion-Weighted Imaging sequences (DWI): Sensitive to the movement of water molecules and can help differentiate lesions based on their cellularity.
- Sweep Imaging with Fourier Transformation sequences (SWIFT): This sequence allows for simultaneous imaging of hard and soft tissues.

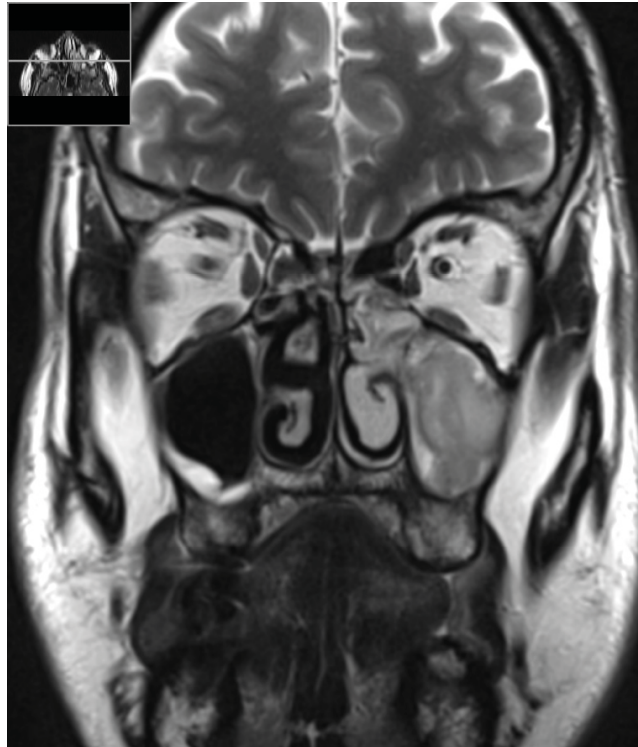


Figure 14: Facial MRI, coronal section sequence T2: tissue thickening of 23 mm of major axis in relation to the left middle meatus with a heterogeneous T2 signal aspect (<https://www.information-dentaire.fr/formations/chech-du-traitement-dune-sinusite-chronique-maxillaire/>)

The choice and optimization of these different sequences, including specific parameters such as repeat time (RT), echo time (ET), cut thickness are essential to obtain images with the contrast and resolution necessary for diagnosis (Chua et al., 2021):

- RT: time interval between the application of two successive radio frequency pulses.
- TE: time between the application of the radiofrequency pulse and the measurement of the echo signal.
- The cutting thickness determines the volume thickness of the imaged tissue, influencing the spatial resolution of this dimension.

A typical MRI protocol for maxillary sinus assessment with different sequences is required to differentiate the causes of clouding (Chua et al., 2021).

II.1.5. Ultrasonography

Ultrasound is based on the use of ultrasound, high-frequency sound waves produced by the piezoelectric effect. Crystals in the probe vibrate under the effect of an electric current,

emitting these inaudible waves that propagate through the tissues. Indeed, the frequency of these ultrasounds, generally between 2 and 20 MHz, is well above the limit audible to humans (20 to 20,000 Hz). When these ultrasounds encounter an interface between two tissues with different acoustic impedances, part of the wave is reflected, forming an echo. The probe, also functioning as a receiver, picks up these echoes and converts them into electrical signals (Hartmann, 2016).

The formation of the ultrasound image depends on the analysis of these echoes. The ultrasound machine measures the time it takes for the echo to return to the probe, which makes it possible to determine the depth of the interface (Hartmann, 2016).

Ultrasound images can be viewed in a variety of modes, including Mode A (Amplitude), which represents echoes as peaks on a graph, and Mode B (Brightness), which represents echoes by points whose brightness varies depending on the intensity of the echo, forming a two-dimensional image (cross-section) (Hartmann, 2016).

The different structures of the human body appear on the ultrasound image with different levels of gray depending on their ability to reflect ultrasound, called echogenicity. Different tissues appear with distinct levels of gray: liquids are usually anechoic (black), homogeneous tissues hypoechoic (medium gray), and heterogeneous tissues, bone and air hyperechoic (light gray to white) (Hartmann, 2016).

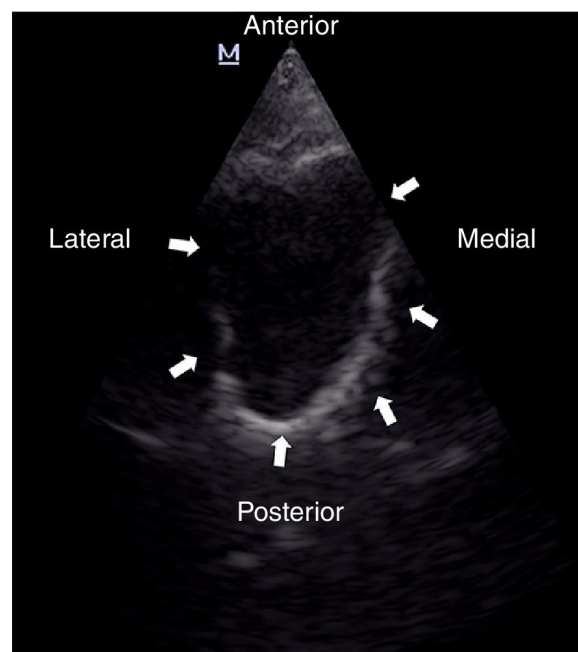


Figure 15: Right maxillary sinus ultrasound (Blanco et al., 2015)

For maxillary sinus ultrasound, probe placement varies between studies:

According to Cheong et al. (2022), the probe is usually placed on the upper jawbone, it is configured in A-mode with a slightly flexion head of the patient and a frequency of 4.5 MHz.

According to Mladina et al. (1994), they also used mode A with a 3.5 MHz probe initially placed perpendicular to the canine fossa and then oriented at different angles.

Karantanas & Sandris. (1997) used 3.5 and 7.5 MHz probes by making sagittal and axial sections, the patient being in supine and erect positions in order to identify the posterior antral wall.

For maxillary sinus examination, ultrasound can detect the presence of fluid.

Under normal conditions, the air contained in the sinus causes reverberation artifacts. In the event of sinus occupancy, for example during sinusitis, the fluid present appears as an anechoic zone, allowing the hyperechoic walls of the sinus to be visualized (Figure 15). (Cheong et al., 2022)

Ultrasound is thus a useful tool for the detection of a maxillary sinus infection which, by being harmless and non-invasive, can, by playing a complementary role, provide additional information than X-rays and potentially avoid the performance of a CT scan (Karantanas & Sandris, 1997).

II.2. The limits of the different imaging techniques

II.2.1. CBCT

A major limitation of CBCT is its limited contrast resolution, which makes it difficult to assess and differentiate between different types of soft tissue (Ginat & Gupta, 2014). Unlike conventional CT, there are no specific "windows" for soft tissues (White & Pharoah, 2008).

CBCT is also very sensitive to artifacts, especially metal artifacts, for example such as amalgam dental restorations or implants that create light or dark trails and degrade image

quality and can potentially obscure fine structures such as the sinus floor (Jacobs & Quirynen, 2014).

Although the radiation dose of CBCT is generally much lower than that of a conventional CT scan, it is significantly higher than that of traditional 2D X-rays such as panoramic or periapical radiographies (White & Pharoah, 2008). The dose also varies considerably depending on the device, the FOV and the exposure parameters (Jacobs & Quirynen, 2014).

Noise and spatial resolution are often managed in a trade-off, since many factors that improve one degrades the other (for example voxel size, reconstruction filter) (Figure 16). Noise in CBCT is often higher than in conventional diagnostic CT owing to a relatively high amount of electronic noise in the detector and other factors (Pauwels et al., 2015).

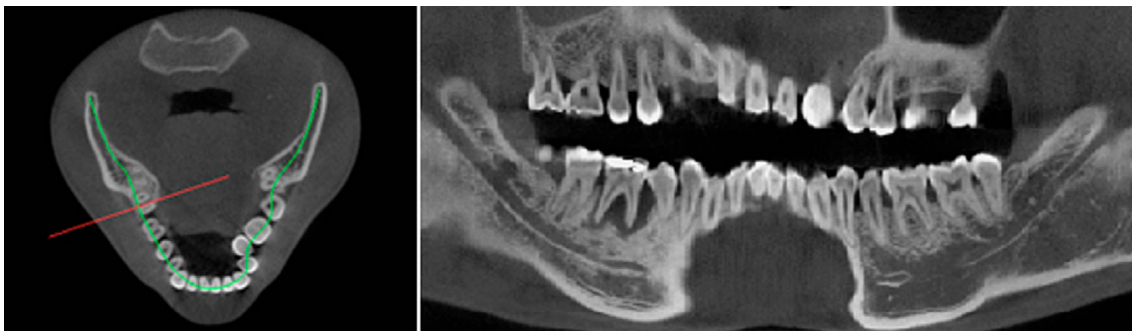


Figure 16: Synthetic panoramic images (right) along a curve drawn in the axial plane (left) (Pauwels et al., 2015)

Finally, during a CBCT acquisition, even for a local indication, the field of view (FOV) can include extensive anatomical structures. The interpretation should extend to the entire volume acquired, not just the original region of interest. The detection of incidental anomalies (such as in the maxillary sinuses) is frequent, which requires specific training and takes time for interpretation (White & Pharoah, 2008).

II.2.2. Panoramic radiography

When it comes to maxillary sinus imaging, panoramic radiography has significant limitations. Although it can provide an overview of this region and is an accessible

imaging technique, its spatial resolution lower than intraoral radiographs and its limited width of the focal trough, especially in the anterior region where part of the maxillary sinus is located, compromise the accurate detection of lesions. Additionally, the superimposition of other anatomical structures, such as the spine, in the anterior region can generate artifacts and obscure important details of the maxillary sinus (MacDonald & Telyakova, 2024).

Panoramic radiography also suffers from inherent problems of distortion of anatomical structures, including a degree of magnification, from 10 to 30% depending on the OPG brand but present on all panoramic radiographs. This makes horizontal measurements of low clinical value (Rushton & Horner, 1996).

The panoramic image is a two-dimensional representation of a three-dimensional structure, which makes it impossible to measure distances in the anterior-posterior direction (Cen et al., 2020). For example, the presence of air between the tongue and the hard palate can lead to a band of overexposure and can hinder the visualization of the maxillary sinus. This is because it creates a dark airspace that can obscure the apical region of the maxillary teeth and reduce the image quality in that area (Rushton & Horner, 1996)(Suparno et al., 2023).

Regarding its clinical use for the evaluation of the maxillary sinus panoramic radiographs are severely limited. Although panoramic X-rays can be used to get an idea of bone depth for implants, inherent inadequacies such as magnification and variable clarity limit its accuracy in assessing critical structures such as the maxillary sinus floor (Rushton & Horner, 1996).

In addition to projection errors, blurred images, which can affect the interpretation of maxillary structures, this technique is considered severely compromised for the detailed evaluation of the maxillary sinus (MacDonald & Telyakova, 2024).

II.2.3. Computed tomography

Although CT scan is a valuable tool in dental imaging to assess the maxillofacial region, including the maxillary sinus, and to aid in the diagnosis of various conditions, they

have significant limitations. A major concern is the radiation dose received by the patient, which is usually higher with computed tomography than with CBCT (White & Pharoah, 2008).

Conventional CT uses a narrow fan beam that rotates around the patient several times in a spiral pattern to cover the area of interest (Figure 17). This scanning technique contributes to increased exposure to ionizing radiation for the patient (White & Pharoah, 2008).

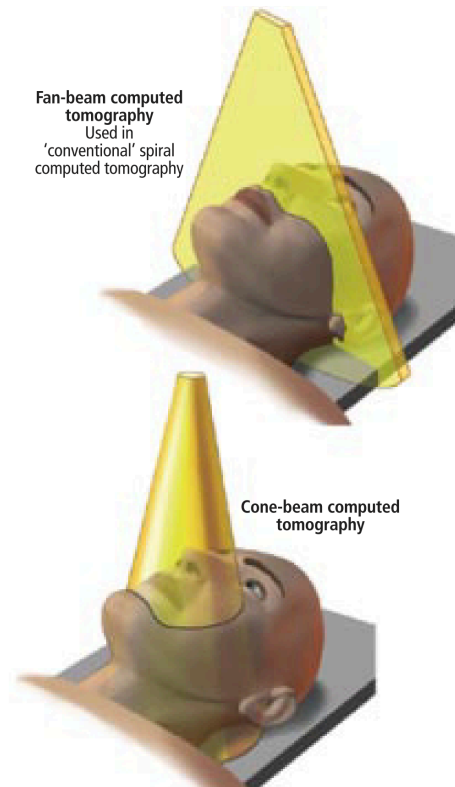


Figure 17: The fan beam upon which spiral computed tomography is based interrogates only a slice of tissue, whereas the cone beam of cone-beam computed tomography interrogates a 3-dimensional region within a 360° rotation (MacDonald-Jankowski & Orpe, 2006).

CT imagery, like CBCT, is prone to metal artifacts caused by high-density objects such as amalgam dental restorations, implants, or root canal filling materials. These artifacts appear as light or dark streaks that can degrade the image quality (Mortazavi et al., 2024). Conventional CT may require the use of intravenous contrast agents to improve the contrast of more vascularized soft tissue entities, such as tumors, which is not the case with MRI for example (White & Pharoah, 2008).

Although conventional CT offers a greater range of contrast resolution and can display soft tissue information, MRI appears to demonstrate higher levels of maxillary sinus incident abnormalities for soft tissue pathologies (Jawahar, 2021).

Conventional CT is generally considered to be more expensive compared to CBCT. However, a major advantage of CT over CBCT is its better contrast resolution, allowing for soft tissue information that is not available on CBCT to be displayed (White & Pharoah, 2008).

II.2.4. MRI

A major disadvantage of MRI is its cost and availability. MRI is generally more expensive than CBCT. In addition, the availability of MRI is more limited than that of CBCT (White & Pharoah, 2008). Regarding the duration of the examination, although the overall scanning time may be short, the total time required for an MRI scanner, including patient preparation, is longer than that required for CBCT (Kiran Kumar et al., 2021).

Since the presence of a strong magnetic field is a fundamental feature of MRI, there are significant risks and limitations (Table 3). This magnetic field can potentially displace ferromagnetic metals. Therefore, MRI cannot be used in patients with implanted metallic foreign objects or medical devices containing ferromagnetic metals, such as cardiac implantable electronic devices, such as pacemakers, such as certain brain aneurysm clips, or ferrous foreign bodies in the eye (White & Pharoah, 2008).

Table 3: Absolute and relative contraindications to MRI (Conroy et al., 2021)

Absolute Contraindications	Relative Contraindications
Cardiac implantable devices (e.g. pacemakers, implantable cardioverter, defibrillators, cardiac resynchronization therapy devices)	Coronary/peripheral artery stents
Metallic intraocular foreign bodies	Programmable shunts
Implantable neurostimulators	Metal airway stent or tracheostomies
Cochlear implants	Intrauterine devices
Implantable drug infusion devices	Ocular prosthesis
Intravascular catheters with metal components (e.g. Swan-Ganz catheters)	Stapes implants
Metallic foreign bodies (e.g. bullets, shrapnel)	Surgical clips or wire sutures
Cerebral artery aneurysm clips	Joint replacements
Magnetic dental implants	Inferior vena cava (IVC) filters
	Harrington rods
	Tattoos less than 6 weeks old

Similarly, MRI is not recommended for use in patients with retainers or orthodontics braces made of ferromagnetic alloys. Although metals used in dentistry for restorations or orthodontics made of ferromagnetic alloys do not move, they can distort the image nearby and cause artifacts. Another aspect related to patient comfort is claustrophobia, which some patients can suffer from when positioned in the tight spaces of an MRI machine (White & Pharoah, 2008;Kiran Kumar et al., 2021).

II.2.5. Ultrasonography

Ultrasound is an imaging technique with many advantages such as its low cost, safety (non-irradiating), non-invasive nature and portability for examinations, but nevertheless has several limitations. These limitations can be technical, patient-related, or operator-dependent (Hartmann, 2016).

A major obstacle for ultrasound is the presence of air. Ultrasound propagates very poorly in the air (Hartmann, 2016). A healthy maxillary sinus is filled with air, which limits visualization beyond the anterior wall and surrounding mucosa, manifesting as an "initial complex" on the A-mode ultrasound (Mladina et al., 1994). Only the presence of fluid or dense tissue can allow ultrasound to pass through and visualize deeper structures like the posterior wall of the sinus (Cheong et al., 2022). A significant limitation, specifically

mentioned for maxillary sinuses, is the possibility of false negative results. If a lesion, such as a cyst or polyp, is not in direct contact with the anterior wall of the sinus, it may not be detected by ultrasound because the ultrasound cannot pass through the air between it and the probe (Mladina et al., 1994).

Finally, ultrasound is a technique that is highly dependent on the operator. It is essential that the operator has a thorough knowledge of anatomy to properly position the probe and scan the area of interest from different angles to minimize artifacts. Technical or interpretive errors are also possible (Hartmann, 2016).

It can play a complementary role with other imaging modalities, such as CT, which may be necessary for a complete and accurate diagnosis, especially in cases of chronic inflammation in case of a detailed anatomical evaluation (Mladina et al., 1994).

II.3. Comparison of the difference techniques

II.3.1. Resolution and Precision

Accurate assessment of the maxillary sinus, particularly in its close relationship to the dentoalveolar region and the planning of surgical procedures close to its floor, requires imaging techniques with high spatial resolution and dimensional accuracy (Yeung et al., 2022).

Unlike two-dimensional X-rays such as panoramic radiography, CBCT permits non-overlapping visualization of the entire acquired volume, which is crucial for assessing the anatomy and pathology of the maxillary sinus (Yeung et al., 2022).

Some manufacturers can adjust other settings that will affect the image quality (Distefano et al., 2023) :

- Pipe current (mAs): the product of current intensity (mA) and exposure time (s). This value allows the netness, clarity and darkness of the image to be adjusted, but therefore plays a role in the patient's dose and exposure.
- Potential difference (kv) at the tube outlet: this parameter quantifies the penetration capacity of the tissues and affects the contrast. High Kv values result in more penetrating X-rays.

- Voxel (μm): it is the constituent element of the three-dimensional physical image. Its size varies depending on the type of imaging performed, but it varies between 0.05mm and 0.4mm. The smaller the size of the voxel, the higher the size of the resolution of the 3D image.

In addition, CBCT's isotropic voxels, of equal dimensions in all three planes, allow a faithful and distortion-free multiplanar reconstruction of the images, guaranteeing linear measurements of high reliability and precision, essential for the pre-surgical evaluation of the bone morphology of the sinus and the thickness of its walls (Kiljunen et al., 2015).

Unlike CT scanning, CBCT has a contrast resolution limited mainly to calcified structures such as bone and lacks the ability to differentiate between various soft tissues, although the interface between soft tissues and air is identifiable (White & Pharoah, 2008).

The CT imagery, is more expensive and involves a higher radiation dose and offers less noise and a wider range of contrast resolution, allowing better visualization and differentiation of soft tissues, which is crucial to assess the extension of certain pathologies (White & Pharoah, 2008).

MRI, on the other hand, excels at soft tissue contrast resolution without using ionizing radiation, although it is more expensive and has contraindications for some metal implants (White & Pharoah, 2008).

Noise refers to the random variability in voxel values in an image. The overall noise of an X-ray image is the sum of the different noises created during the stages of image formation (Figure 18). There are different sources of noise in radio-graphic images, mainly (Pauwels et al., 2015):

- Quantum noise: caused by the inherent random nature of the interactions happening during X-ray production and attenuation
- Electronic noise: caused by the conversion and transmission of the detector signal.

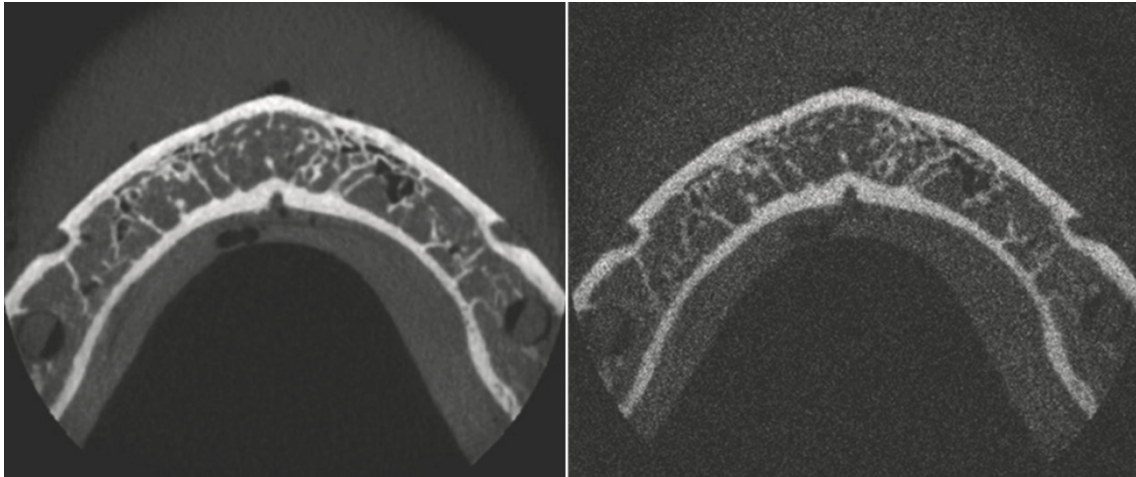


Figure 18 : Artificial increase in image noise (Pauwels et al., 2015)

II.3.2. Radiation Exposure

The dose received by a patient during a CBCT examination for the facial skeleton is a matter of concern, as it represents additional exposure to X-rays. The effective dose, measured in Sievert (Sv) or more commonly in milli-Sievert (mSv) or micro-Sievert (μ Sv) in practice, is used to assess the potential risk to the human body (Li, 2013).

For comparison, a single periapical X-ray has an effective dose of about 5 μ Sv, while a standard panoramic X-ray ranges from 2.7 to 24.5 μ Sv. The actual doses reported for CBCT vary widely, including depending on the device and protocols used. The general values for CBCT range from 10 to 1000 μ Sv, with specific ranges depending on the FOV used. Some indicate that the dose of a CBCT should ideally be equivalent to 2 to 10 panoramic X-rays (between 20 to 100 μ Sv) (Kunzendorf et al., 2021)

In contrast, the effective doses reported for CBCT of the facial skeleton vary widely across studies, with ranges from (Al-Okshi et al., 2015):

- FOV of 5 cm high: 9.7 μ Sv to 197.0 μ Sv
- FOV heights between 5 and 10 cm: 3.9 μ Sv to 674.0 μ Sv
- FOV >10 cm: 8,8 μ Sv to 1073,0 μ Sv

Compared to CT scans, the effective dose of CBCT is usually much lower, with CT doses reported to be about several to ten times higher than those of CBCT (Li, 2013)

Table 4: Comparison of radiation dose from different techniques from the Federal Nuclear Control Agency (<https://afcn.fgov.be/fr/dossiers/applications-medicales/comparaison-des-doses-de-rayonnements>)

Sources of radiation	Dose in millisievert	Natural exposure time required to reach the same dose
Conebeam CT	0,2 mSv	1 month
Panoramic radiograph	0,01 mSv	2 days
CT-scan of the sinuses	0,1 mSv	15 days
Periapical radiography	0,005 mSv	1 day
PET-scan	4,5 mSv	2 years
4 hours of flight	0,005 mSv	1 day
Natural radiation on earth	2,4 mSv	1 year

The effective dose of a CBCT test is closely related to the FOV used, exposure parameters (such as kVp, mAs, and voxel size), the type of CBCT device, and even the positioning of the FOV. Wider FOV results in a higher radiation dose (Li, 2013).

The average annual exposure to natural radiation is about 2.4 mSv (or 2400 μ Sv) (Table 4), which allows the doses of CBCT examinations to be put into perspective (Jacobs & Quirynen, 2014)

Optimizing the radiation dose of CBCT is a key factor. Indeed, the selection of a FOV appropriate to the clinical indication is necessary because the size of the FOV has a negative impact on the radiation dose to the patient. The ALARA "As Low As Reasonably Achievable" and ALADA "As Low As Diagnostically Acceptable" principles recommend the use of the smallest FOV that provides sufficient diagnostic information. Reducing the size of the FOV is an important strategy to minimize radiation exposure (Kiljunen et al., 2015).

II.3.3. Artifacts and Limitations

CBCT artifacts are abnormal signals that degrade image quality and can complicate diagnosis. They do not correspond to anatomical reality and are the result of the conditions of acquisition or the device itself (Olszewski, 2020).

There are different types of artifacts identified:

- Aliasing Artifact (Figure 19): This is a technical artifact related to the CBCT device itself. Although it may be visible in the soft tissues around the bone, its presence is mainly related to the quality of the detectors. Improving these components helps to reduce it (Olszewski, 2020).



Figure 19: Axial view of mandible and cervical vertebra. Thick arrows: aliasing artefact (Olszewski, 2020)

- Ring Artifact (Figure 20): Appears as concentric rings centered around the aircraft's axis of rotation. They are more pronounced when homogeneous media are imaged, such as the soft tissues of the oral floor. Their presence usually indicates a problem with the calibration of the CBCT device or defective detector elements (Olszewski, 2020).

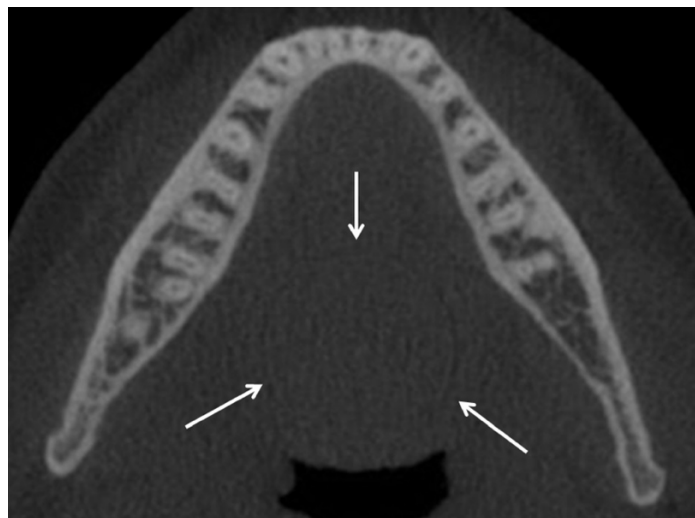


Figure 20: Axial view of mandible. Arrows: ring artifact visible in the middle of the mouth floor (Olszewski, 2020)

- Beam hardening artifacts (Figure 21): Caused by the presence of materials such as metals (amalgam fillings, implants, crown bridges or intermaxillary fixations screws) They appear as dark or light bands (streaks) and can obscure the surrounding anatomy and make evaluation difficult (Olszewski, 2020).

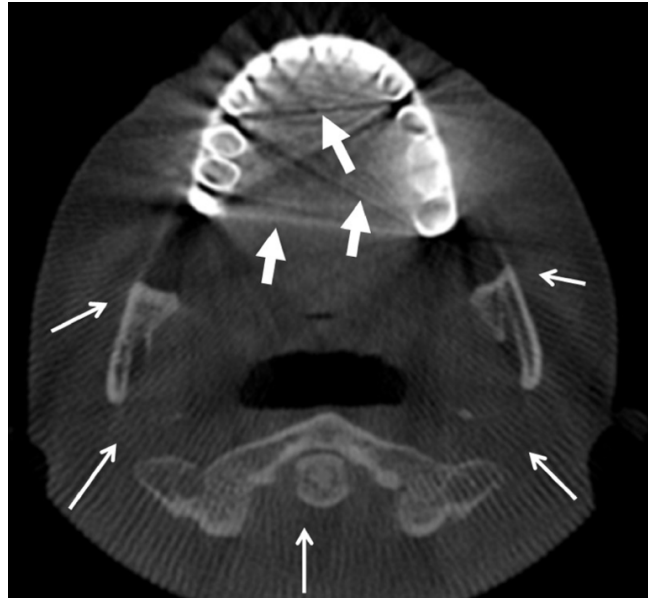


Figure 21: Axial view of mandible and of cervical spine. Thick arrows: complex pattern of streaks due to crowns and bridge present on all upper teeth. Thin arrows: aliasing artifact (Olszewski, 2020)

Other artefacts called movement artefacts can be involved, in particular due to a mispositioning of the patient, a displacement or a movement of the patient's jaw during the scan, as it lasts a relatively long time between 15 and 20 seconds. CBCT is more sensitive to that than conventional CT (De Marneffe, 2017). These movements can cause the image to become blurred or double images to appear (Jacobs & Quirynen, 2014).

Indeed, for the execution of an X-ray examination or a CBCT it involves several procedures, generally the patient is positioned standing or sitting, can position his hands or not on supports in front of him depending on the type of device (Figure 22). He must maintain a stationary position, as stable as possible, avoid swallowing and making too much breathing movements. A CBCT compared to a panoramic radiography, does not require any other special preparations, apart from removing all the glasses, earrings, piercings and other metal objects that could hinder the visualization of the image with the appearance of artifacts (Abramovitch & Rice, 2014).



Figure 22: Different types of CBCT gantries. Left: seated patient position (3D Accuitomo® 170; J. Morita, Kyoto, Japan). Right: standing patient (WhiteFox®; Acteon Group, Merignac, France)

II.3.4. Costs and Accessibility

For the evaluation of the maxillary sinus, the choice of an imaging technique involves a trade-off between diagnostic performance, costs, accessibility and completion time (Abramovitch & Rice, 2014). Conventional two-dimensional methods are by far the most accessible and least expensive in a standard dental practice, with very short scan times (Jacobs & Quirynen, 2014).

Compared to medical CT, CBCT is generally less expensive to acquire and maintain. CBCT scan times can be short, sometimes comparable to those of a panoramic radiography, which contributes to its effectiveness (Jacobs & Quirynen, 2014).

The accessibility of CBCT is increasing, but it remains less than that of 2D. In contrast, medical modalities like CT and MRI are generally less accessible and more expensive in a dental setting because they are not available in community practices (De Marneffe, 2017).

On the other hand, the cost of setting up a CBCT must also be taken into account. Early CBCT devices were often limited to a single FOV size. Nowadays, contemporary scanners offer different range of FOVs depending on the area you want to diagnose. The cost of radiography was initially related to the size of the detector and the power of the X-ray generator for imaging denser regions with larger FOVs. A bi-maxillary CBCT will therefore be more expensive for the patient than a maxillary CBCT (Abramovitch & Rice, 2014).

Thus, for indications involving mainly the evaluation of bone and dental structures related to the sinus, a dedicated CBCT often offers the best diagnostic cost/effectiveness balance compared to CT or MRI, even if panoramic or retroalveolar radiographs, despite their limitations, can sometimes provide a quick and inexpensive first indication (Figure 23) (Jacobs & Quirynen, 2014).

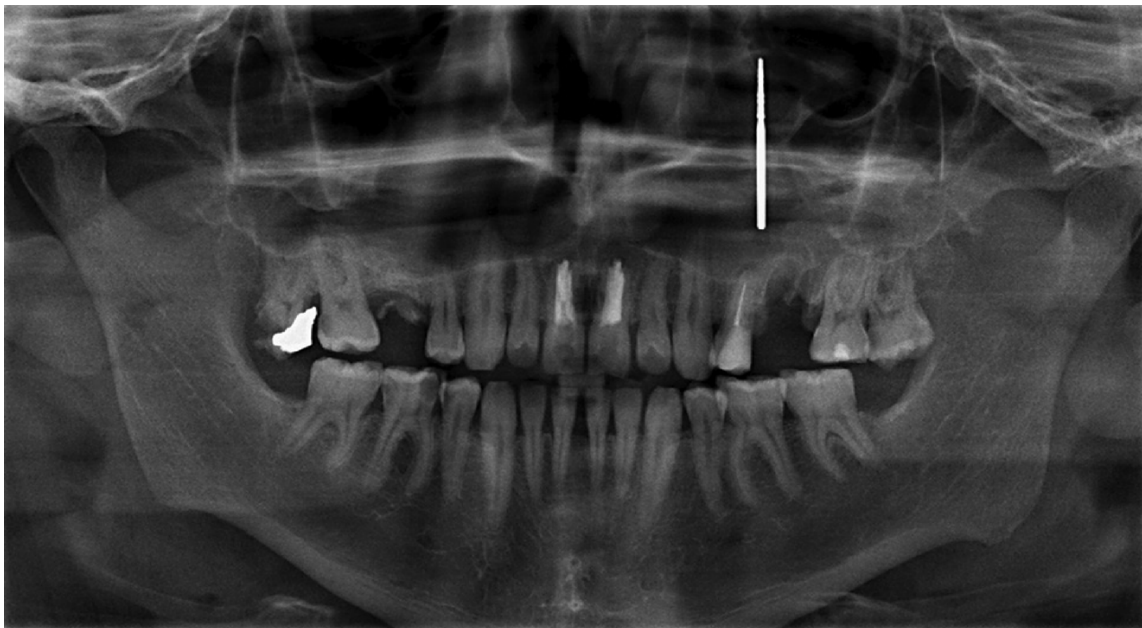


Figure 23: A straight burr impinged into the left maxillary sinus (Tilaveridis et al., 2022)

II.3.5. Safety and radioprotection

Patient safety and radiation protection are a crucial aspect of the use of CBCT, especially due to exposure to ionizing radiation. Increasing the dose to the patient during a CBCT examination is a major concern, especially for pediatric patients who are more radiosensitive (Shin et al., 2014).

The guiding principles of radiation protection are ALARA (As Low As Reasonably Achievable), which aims to keep the dose as low as reasonably possible, and ALADA (As Low As Diagnostically Acceptable), which focuses on maintaining a dose low enough to minimize risk while ensuring that the image is of sufficient quality for diagnosis. More recently, the ALADAIP principle (As Low As Diagnostically Acceptable being Indication-oriented and Patient-specific) has been proposed to include orientation towards the specific clinical indication and adaptation to the individual (Yeung et al., 2022).

It is therefore essential to implement measures to reduce this dose without compromising the necessary diagnostic quality. Among the methods of radiation protection, the use of shielding devices is relevant. Wearing a leaded apron or thyroid protection can reduce the dose received by some organs, although its usefulness is debated if the organ is not directly in the main bundle (Li, 2013).

Studies have examined the effectiveness of leaded thyroid collars for thyroid gland protection and leaded glasses for lens protection (Li, 2013). Indeed, the use of thyroid collars, shows a reduction in thyroid dose (ranging from 61% to 72% depending on the FOV) and a significant dose reduction of more than 60% through the use of leaded glasses, without negatively affecting image quality in clinically relevant areas for dental imaging (Li, 2013).

Beyond shielding, optimizing the CBCT scanning protocol is fundamental and even the most important to minimize dose. Children are also more radiosensitive than adults. It is therefore particularly important to optimize parameters (especially kVp) and limit FOV when imaging younger patients (De Marneffe, 2017). This involves choosing the most suitable field of view (FOV) for the diagnostic task, as well as adjusting other exposure parameters such as kVp, mAs or voxel size (Al-Okshi et al., 2015)

III. Role of the CBCT in Maxillary Sinus Pathologies

III.1. Diagnosis of Maxillary Sinus Pathologies

III.1.1. Maxillary sinusitis: Dental or non-dental origin

Maxillary sinusitis is a common inflammatory and/or infectious condition that affects the maxillary sinus. Due to the close proximity between the roots of the posterior maxillary teeth and the floor of the maxillary sinus, dental pathologies are a common cause of maxillary sinusitis (Gilain & Laurent, 2005). It is therefore crucial to distinguish between sinusitis of dental origin (odontogenic) and sinusitis of non-dental origin (rhinogenic, fungal or due to a foreign body) for an accurate diagnosis and appropriate treatment plan (Fricain, 2014).

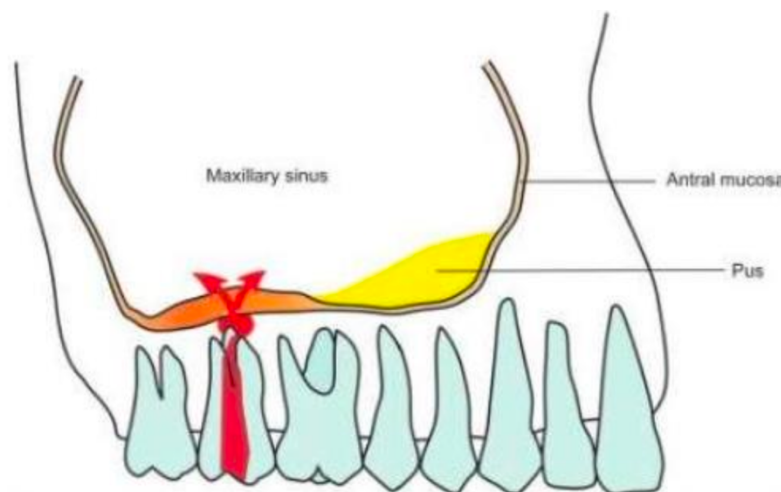


Figure 24: Multiplication of bacteria invading from the focus of a dental infection results in odontogenic (Sumathy & Muthiah, 2020).

The causes of maxillary sinusitis are varied. The most common include infections resulting from cavities, leading to pulp necrosis and periapical pathology (Figure 24). Advanced periodontal involvement can also be an important etiological factor. Dental maxillary sinusitis accounts for about 40% of maxillary sinusitis cases (Psillas et al., 2021). Iatrogenic factors are also often involved, including oral-antral communications secondary to complicated tooth extractions or cystic curettages, migration of root canal filling materials into the sinus, or displacement of dental implants or root fragments in the sinus cavity. These foreign bodies can act as local irritants and promote infection (Figure 25) (Jawahar, 2021).

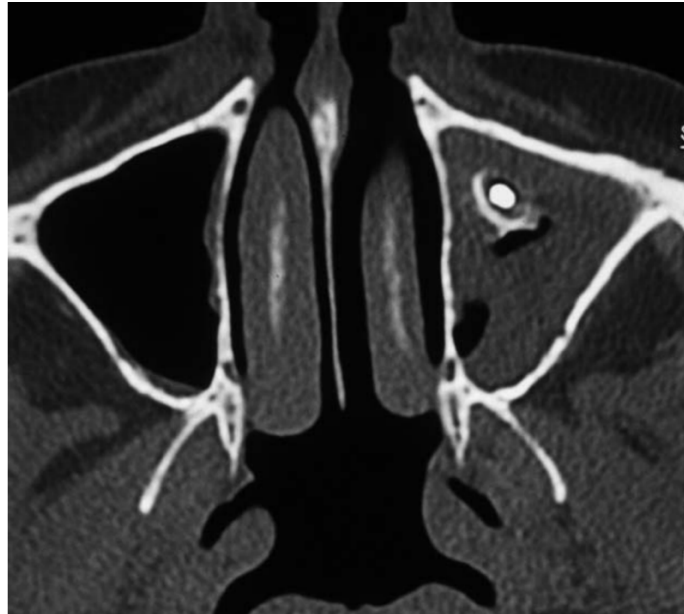


Figure 25: CT scan, axial section: incomplete opacity of the lower left maxillary sinus with foreign body image (Gilain & Laurent, 2005).

There are also many non-dental causes of maxillary sinusitis. Rhinogenic origin is very common, often following an acute viral infection of the upper respiratory tract (Gilain & Laurent, 2005). Obstruction of the ostium of the maxillary sinus, the point of drainage to the middle meatus, by inflammatory edema, polyps, or morphological abnormalities, plays a major role in sinusitis of rhinogenic origin (Gilain & Laurent, 2005). Fungal infections, especially those caused by *Aspergillus* spp, are another non-dental etiology, sometimes associated with the presence of foreign bodies in the sinus (Bell et al., 2011).

Clinically, the symptoms of maxillary sinusitis, whether dental or not, can overlap, making differentiation difficult. Imaging is essential to confirm the diagnosis of maxillary sinusitis and determine its etiology (Premoli Maciel et al., 2020).

Conventional radiographs, such as panoramic radiograph, may reveal opacification of the maxillary sinus or the presence of foreign bodies (Jawahar, 2021).

However, panoramic radiography is a two-dimensional image whose limitations often do not allow for a precise assessment of the anatomical relationship between the dental apex and the sinus floor, or the bone or mucosa (Premoli Maciel et al., 2020).

This is where the role of CBCT becomes particularly important in the etiological diagnosis of maxillary sinusitis, especially to identify a dental origin (Premoli Maciel et al., 2020).

It excels in the precise identification of radiological signs of maxillary sinusitis of odontogenic origin, such as thickening of the sinus mucosa (Figure 26). Indeed, CBCT often makes it possible to observe a localized thickening of the mucosa in front of a pathological tooth, suggesting an extension of the dental infection. A thickening of the sinus mucosa greater than 1.0mm is considered significant (Premoli Maciel et al., 2020).



Figure 26: Odontogenic sinusitis with opacification of the right maxillary sinus as a result of a dental infection (coronary, sagittal, axial views) (Langlais et al., 2009)

III.1.2. Cysts and pseudocyst

Cysts and pseudocysts of the maxilla, although very varied in their etiology, diagnosis and course, share the needs for surgical treatment. When they present superinfection or a significant increase in volume resulting in dysfunctions, deformities or a risk of fracture (Ruhin et al., 2005).

The discovery and identification of these lesions require a rigorous diagnostic evaluation, based on clinical and radiographic arguments (Ruhin et al., 2005). CBCT has established itself as an essential imaging tool for the analysis of cysts in this part of the maxillary sinus. It makes it possible to visualize their presence, their number, their precise location

(floor, walls, roof of the sine) and their dimensions in the three planes of space (Yeung et al., 2018).

Among cystic conditions, mucosal retention cysts (also known as maxillary sinus pseudocysts or antral pseudocysts) are the most common manifestations due to inflammatory changes in the Schneiderian membrane (Figure 27) (Yeung et al., 2018). They result from inflammation of the sinus mucosa leading to obstruction of the ducts of the small mucous glands (Hung et al., 2021).

They typically appear as a homogeneous, dome-shaped opacity, with no visible cortical coating, extending towards the lumen of the maxillary sinus and attached to the bone wall (Yeung et al., 2018).

Although the association between mucosal retention cysts and dentoalveolar pathology is debated, the CBCT showed that sinuses with associated endodontic or periapical lesions had a higher probability of mucosal retention cysts located on the sinus floor, and that these cysts were slightly larger in these cases (Hung et al., 2021).

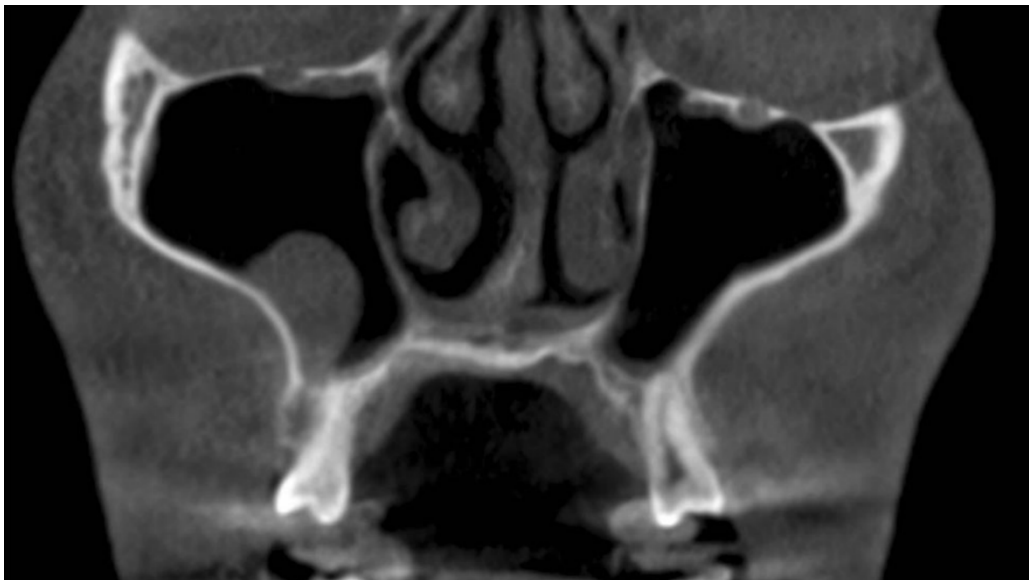


Figure 27: CBCT image of a patient with a mucous retention cyst that was diagnosed at the lateral wall of the right maxillary sinus (Yeung et al., 2018)

Radicular cysts are inflammatory lesions of dental origin, resulting from the cystic transformation of an apical granuloma. They account for almost the majority (nearly 60%) of cystic lesions of the maxillae. Although the extension of a radicular cyst into the

maxillary sinus is less common, when it occurs, it can cause sinus opacity, sometimes mistaken for simple sinusitis. CBCT is essential for making the diagnosis in those cases (Bassou et al., 2007).

CBCT typically reveals a well-defined, fluid-density cystic formation appended to the apex of a tooth (often necrotic or extracted) and developed inside the maxillary sinus (El Kettani et al., 2011). A key feature visualized on CBCT is the presence of a thin, dense border of bone density that limits the cyst and continues with the lamina dura of the causal tooth (Figure 28). This border corresponds to the bony floor of the maxillary sinus which has been pushed upwards by the voluminous cyst, creating an appearance of "double bottom" on axial sections or "double ceiling" on frontal reconstructions (Bassou et al., 2007). CBCT makes it possible to assess the relationship of the cyst with the ducts of the teeth, the appearance of the bony cortical and its precise extension within the sinus (El Kettani et al., 2011).

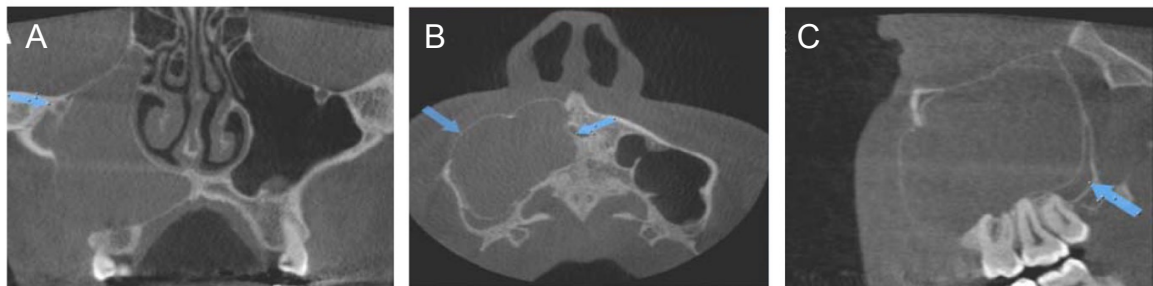


Figure 28: Cone-beam computed tomography (CBCT) scans of the radicular cyst in the maxillary sinus. A- The coronal view clearly shows the right maxillary sinus filled with cyst in the proximity to the infraorbital canal and the floor of the orbit; B - The axial view clearly shows the cystic lesion in the maxillary sinus, with thinning and perforation of the cortical plate on the medial aspect of the maxilla; C- The sagittal view of the maxilla shows the expansive lesion with posterior growth in the maxillary tuber (Biocanin, 2015)

III.1.3. Malignant and benign tumors

Various benign tumors can affect the maxillary sinus. These include osteoma, inverted papilloma, or ameloblastoma or odontogenic keratocyst (Bell et al., 2011). Although benign, some of these lesions may present local aggression and a potential for recurrence (Ruhin et al., 2005). The presence of big air spaces within the sinus allows the asymptomatic development of sinus tumors. At the premature stages, these tumors are often asymptomatic or imitate inflammatory diseases, leading to a delay in diagnosis or misdiagnosis (Ali et al., 2015).

Odontogenic keratocyst, for example, has a reputation for recurrence requiring more aggressive treatment than for other cysts, and an extensive form may have a therapeutic approach that can be superimposed on that of aggressive osteolytic lesions such as ameloblastoma (Ruhin et al., 2005).

Ameloblastoma is a well-known osteolytic lesion. It is a benign tumor but endowed with a singular aggressiveness by its extensive and recurrent character. Imaging, including CBCT, is essential to assess the extent of these lesions and their impact on adjacent structures (Ruhin et al., 2005).

A rare but notable entity is inflammatory pseudotumor of the maxillary sinus. Benign in nature, it is often characterized by aggressive clinical behavior with lytic power that can mimic a malignant tumor. CBCT imaging is crucial in this case and typically shows a dense and homogeneous tissue process in the maxillary sinus with erosion of the bone walls and possible extension to adjacent structures such as the ipsilateral nasal cavity (Fricain, 2014).

Finally, osteoma is a benign osteoformative tumor. Imaging evaluates its volume, its location, and the bone quality. Maxillary damage is less frequent and often smaller. CBCT makes it possible to visualize this dense bone formation (Ruhin et al., 2005).

For malignant tumors, the nasal cavities, and particularly the maxillary sinus, can be the site of carcinomas, mainly squamous cell and adenocarcinomas (Bell et al., 2011).

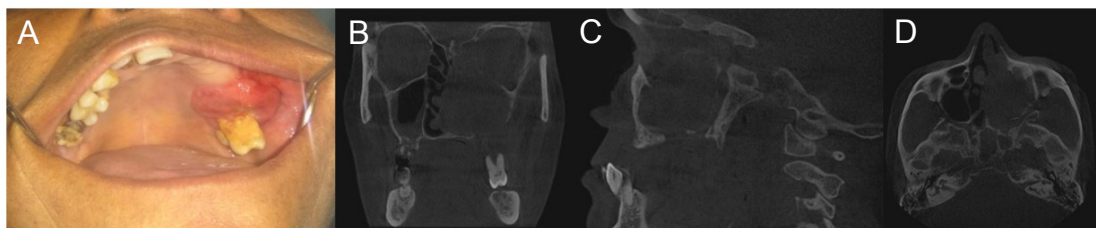


Figure 29: Sinusal carcinoma seen at the CBCT. A - Proliferative growth seen on the alveolar mucosa of left side of maxilla; B - Coronal section of the CBCT; C - Sagittal section of the CBCT (left side); D - Axial section of the CBCT. (Ali et al., 2015)

The axial, coronal and sagittal views obtained by this CBCT highlighted an expansive lesion occupying the entire left maxillary sinus. Nearby structures were destroyed,

including the left lateral wall of the nasal cavity, the left infraorbital rim, the maxillary alveolar bone, the palate and the walls of the maxillary sinus itself. The lesion also extended to the ethmoid and sphenoidal sinuses. The CBCT examination confirmed the involvement of the walls of the left maxillary sinus, in favor of carcinoma with invasion of the left nasal cavity and hard palate (Figure 29) (Ali et al., 2015).

Those cancers can develop from the bone or cartilage supporting tissues, but especially from the overlying mucosa of the nasal and sinus cavities (Bell et al., 2011).

CBCT, often supplemented by MRI in the assessment of malignant tumors, plays a decisive role in their evaluation. It makes it possible to visualize the tumor mass (often unilateral in the maxillary sinus), to identify the presence of bone destruction, which is a key criterion of aggressiveness (Darouassi et al., 2015).

It also permits the definition of apparent tumor boundaries and the assessment of extension to adjacent structures such as the bony walls, floor, roof of the sinus, nasal cavity (via the ostium or medial walls), palate, or orbit (although MRI is preferred for orbital contents) (Maingon, 2001)

III.1.4. Maxillary Sinus fractures

The maxillary sinus, due to its anatomical position in the center of the face, is frequently affected in fractures of the middle facial skeleton. The aeration of the paranasal sinuses weakens the mediotemporal skeleton and can therefore lead to traumatic injuries. Fractures of bone walls and tears in the mucosal surfaces of the maxillary sinus are common in patients with mediotemporal trauma. They can result from an isolated direct impact or be associated with more extensive facial fractures (Ellis & Potter, 1999).

The anterolateral wall of the sinus is the most common site of isolated fractures, often resulting from a direct impact or blow to the zygoma. These fractures can be linear or comminuted, with bone fragments sometimes displaced, and can extend to the orbital rim. An important associated clinical sign may be subcutaneous emphysema of the cheek (Ellis & Potter, 1999).

There are cases of isolated fractures of the posterior wall of the maxillary sinus. One hypothesis proposes that these fractures of the posterior wall result from the impact of the ipsilateral mandibular coronoid process against this wall during facial trauma, often associated with a dislocation or mandibular fracture (Simonds et al., 2011).

Finally, fractures of the alveolar portion of the sinus floor occur more frequently during dental procedures such as exodontia such as third molar extraction rather than shock or impact. CBCT imaging can identify the presence of fracture lines and often fluid effusion, mucosal thickening in the sinus, or partial or complete opacification of the sinus (Figure 30) (Ahmed et al., 2023).

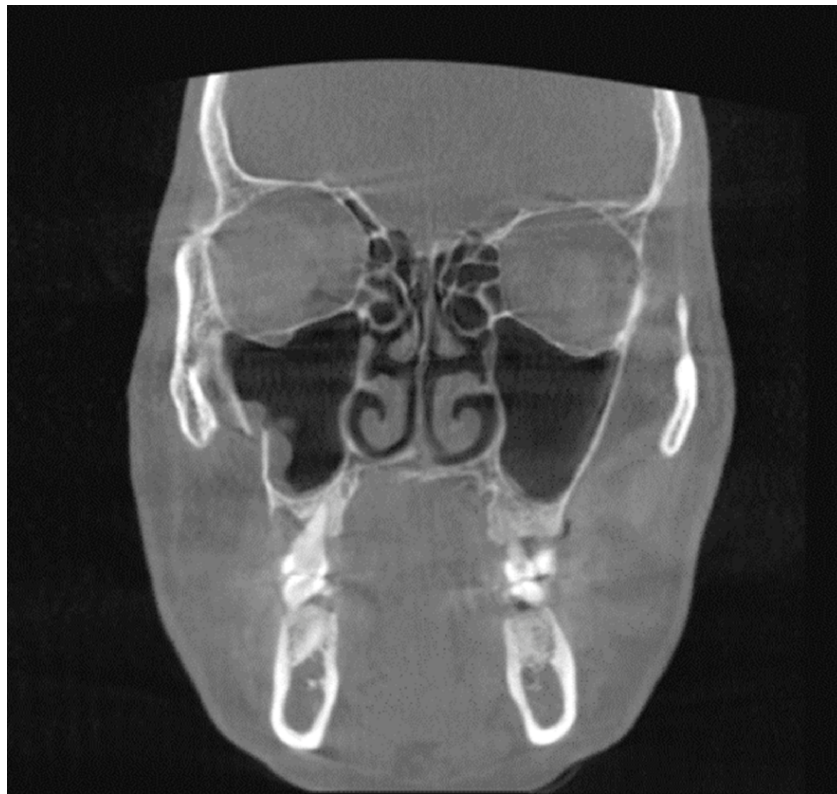


Figure 30: View from the Coronal plane. The CBCT shows a fracture line along the floor of the maxillary sinuses (Ahmed et al., 2023).

The maxillary sinus is a central element of the middle facial mass, and therefore potentially involved in any midfacial fracture. Among the most common associated fractures are fractures of the zygomatico-maxillary complex, fractures of the internal orbit (involving the floor of the orbit), and Le Fort fractures which classify fractures of the maxilla according to their horizontal level (Mclaren et al., 2020).

III.1.5. Oral-sinus communication

Oro-antral communication (OAC) is defined as an open, pathological connection between the oral cavity and the maxillary sinus. This is quite common in oral surgery, especially after the upper first molars are removed, followed by the second molars, third molars, and premolars (Debnath et al., 2025).

OAC can also occur as a result of other dental procedures such as implant dislocations, dehiscence after implant failure, dental or sinus infections compromising bone structure, facial trauma, pathological lesions in the sinus (cysts, tumors), or surgical procedures such as Le Fort osteotomies or the Caldwell-Luc procedure (Dipalma et al., 2025).

The Caldwell-Luc procedure (Figure 31) is a surgical technique that was historically used to treat chronic sinusitis. The traditional technique involved a wide intraoral opening of the anterolateral wall of the sinus, with much of the sinus lining removed. However, it is now considered too invasive and not always effective (Dipalma et al., 2025).

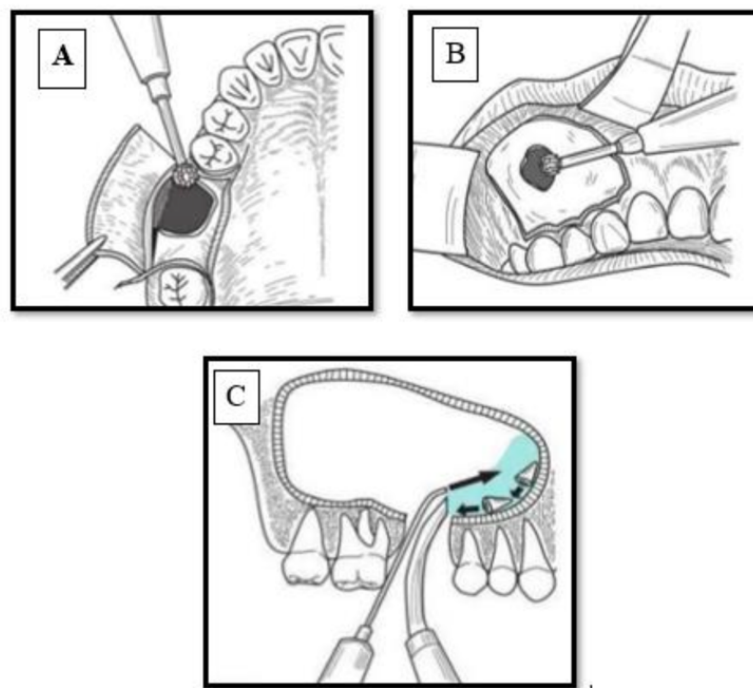


Figure 31: The Caldwell - Luc procedure. A - If a root or foreign body enters the sinus, the socket is widened buccally after lifting a mucoperiosteal flap ; B - A small opening is made in the bone, 1 cm above the first premolar apices ; C - Saline is injected into the sinus, then suction is applied via the socket or the opening (Sumathy & Muthiah, 2020).

The development of an OAC can lead to various complications, affecting the functionality of the maxillary sinus and oral cavity. If an OAC is not diagnosed and managed properly, there is a risk of developing an Oro-antral fistula (OAF). It corresponds to a more advanced stage of the pathological process compared to an OAC. An OAF develops when an OAC fails to close spontaneously, remains open, and epithelializes (Debnath et al., 2025) & (Dipalma et al., 2025).

Maxillary sinusitis is a common complication of OAC, often manifesting within 48 hours for 50% of patients, and within two weeks for 90% of patients if left untreated (Khandelwal & Hajira, 2017).

The diagnosis of OAC is based on a detailed clinical evaluation and radiographic examinations. During the intraoral examination, signs such as the passage of air or liquids between the mouth and nose may be observed (Dipalma et al., 2025).

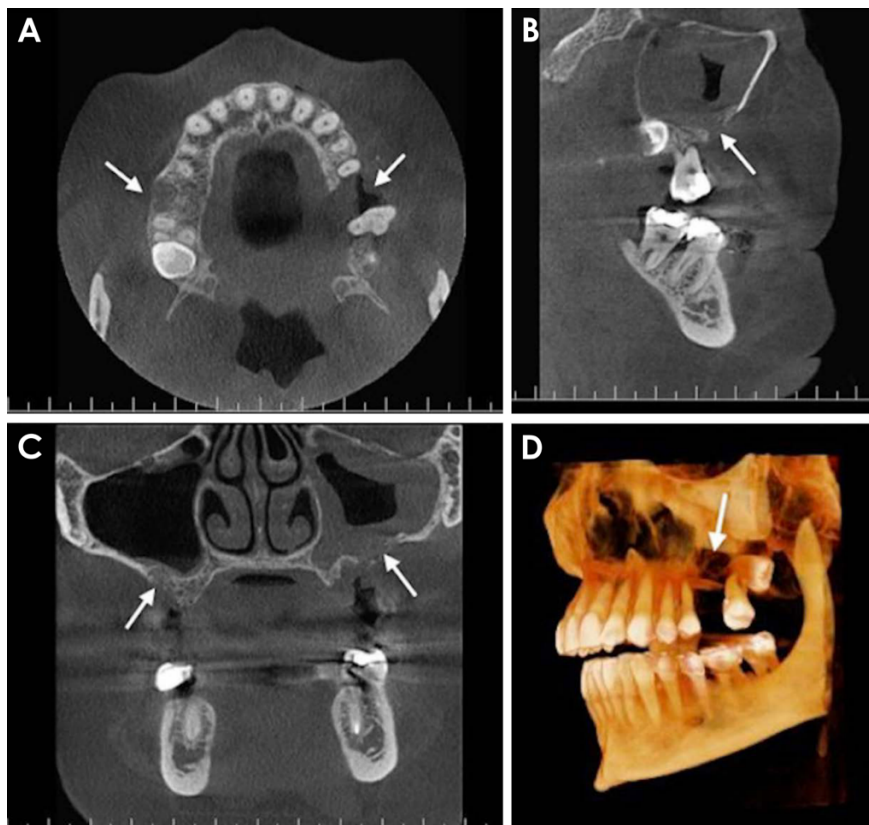


Figure 32 : Multiplanar reformatted cone-beam computed tomographic images of a oral-sinus communication. A- Axial view shows loss of the buccal cortical plate in the right maxillary first molar extraction site and loss of both buccal and lingual cortical plates in the left maxillary first molar extraction site ; B - Sagittal view shows loss of cortication in the left maxillary sinus ; C - Coronal View shows the extraction sockets ; D - A volume-rendered image shows the loss of the cortical plate at the left maxillary first molar's extraction site (Shahrou et al., 2021).

CBCT is the preferred imaging tool for more accurate assessment of OAC (Dipalma et al., 2025). It is ideal for assessing the extent of communication and the size of the defect, the condition of the Schneider's membrane (Figure 32), whether there is thickening or not and visualizing potential foreign bodies in the sinus (Shahrou et al., 2021).

III.2. CBCT-guided Therapeutic Choices

III.2.1. Surgical planning

The surgical planning of procedures that include the maxillary sinus, and in particular bone grafting, dental implant placement or procedures to recover displaced foreign bodies, is greatly improved by the use of CBCT (Rahpeyma & Khajehahmadi, 2015).

Insufficient bone height between the ridge and the sinus floor of less than 5 mm is an indication for an "open" sinus elevation procedure (lateral window approach). A residual height of 10 mm or less usually indicates the need for a sinus lift procedure (Alshamrani et al., 2023).

CBCT helps determine the thickness of the Schneider membrane lining the sinus. A normal membrane thickness is usually less than 1 mm (0.3-0.9 mm). Mucosal thickening of more than 2 mm is considered pathological (Bornstein et al., 2017). Any maxillary sinus sinusitis should be treated prior to sinus lift surgery. Although very thin membranes (less than 1 mm) are susceptible to perforation, the lowest rate of perforation is observed when the thickness is 1.5 to 2 mm. A thickness exceeding 5 mm may be associated with obstruction of the sinus ostium (Alshamrani et al., 2023).

Identifying the pathway, position, and diameter of the alveolar-antral artery (anastomosis between the infraorbital artery and the posterior superior alveolar artery) through CBCT is crucial. An artery with a diameter greater than 0.5 mm can be seen on CBCT images, and significant bleeding should be anticipated if the diameter exceeds 3 mm. Hemorrhage due to injury to this artery is the second most common complication after perforation of the membrane depending on sinus lift procedures (Alshamrani et al., 2023).

The distance between the lateral and medial walls of the maxillary sinus, as well as the angle formed by these structures, are important. Very narrow or very wide sinuses, or with an acute angulation, can complicate the surgery (Alshamrani et al., 2023).

III.2.2. Maxillary sinus floor augmentation (sinus lift)

In the case of advanced atrophy of the posterior maxillary alveolar ridge, insufficient for the insertion of dental implants, the method of choice to restore bone volume is surgical elevation of the maxillary sinus floor, commonly known as sinus lift. This pre-prosthetic operation aims at creating an appropriate bone height and width for osseointegration of the implants (Kiljunen et al., 2015). It can be performed in a single step, with simultaneous placement of the implants, or in two steps, where the graft is placed first, followed by implant insertion after bone maturation (Alshamrani et al., 2023).

There are two main surgical methods for performing a sinus lift, either the lateral window approach (open technique) or the trans-alveolar approach, known as the crestal technique, which is a closed osteotomy technique (Alshamrani et al., 2023).

The lateral window technique (Figure 33) described in the 70s by Tatum is most often performed, especially when the residual bone height is less than 5 mm or in the case of major bone deficits (Matern et al., 2016).

This technique involves the surgical creation of a bony window (osteotomy) in the lateral wall of the maxillary sinus (Alshamrani et al., 2023). Through this opening, the Schneider membrane lining the inside of the sinus is delicately dissected and raised in an apical direction, taking care to preserve its integrity. The space created between the elevated membrane and the original sinus floor is filled with bone graft material (Carrao & DeMatteis, 2015). This technique allows a gain in vertical bone height of more than 9 mm in cases of significant deficits. Osteotomy can be performed using a high-speed handpiece or piezoelectric instruments. The use of piezoelectric instruments is suggested to reduce the risk of perforation of the membrane (Alshamrani et al., 2023).

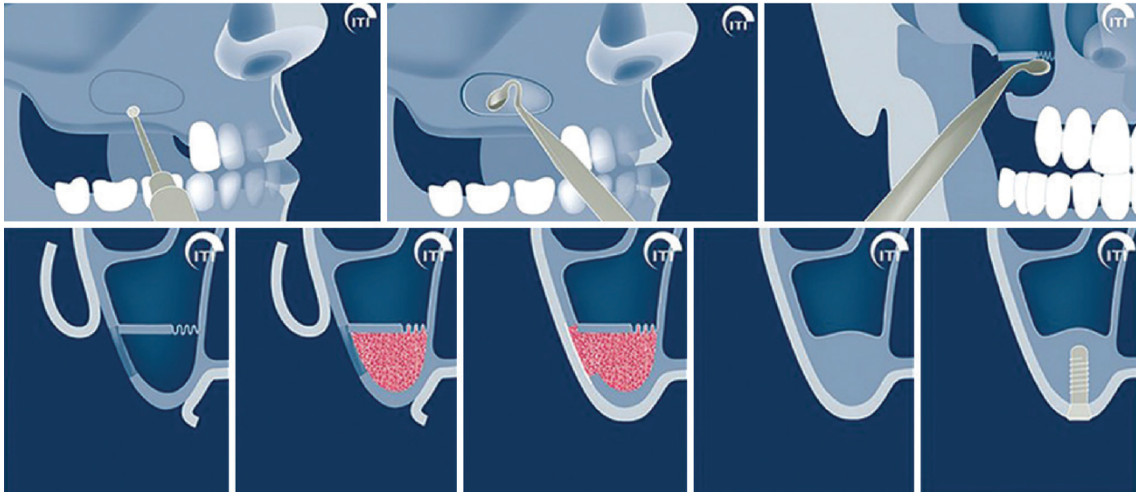


Figure 33: Lateral window approach for sinus augmentation (George et al., 2020)

Then, the trans-alveolar approach (Figure 34) or also known as a crestal sinus lift is usually preferred when the residual bone height is greater than 5 mm (Alshamrani et al., 2023). It is considered less invasive than the lateral approach. It involves the elevation of the Schneider membrane by instruments inserted through the implant site. (Matern et al., 2016). This technique may be less suitable when the need for an increase is great, like more than 3 mm (Carrao & DeMatteis, 2015).

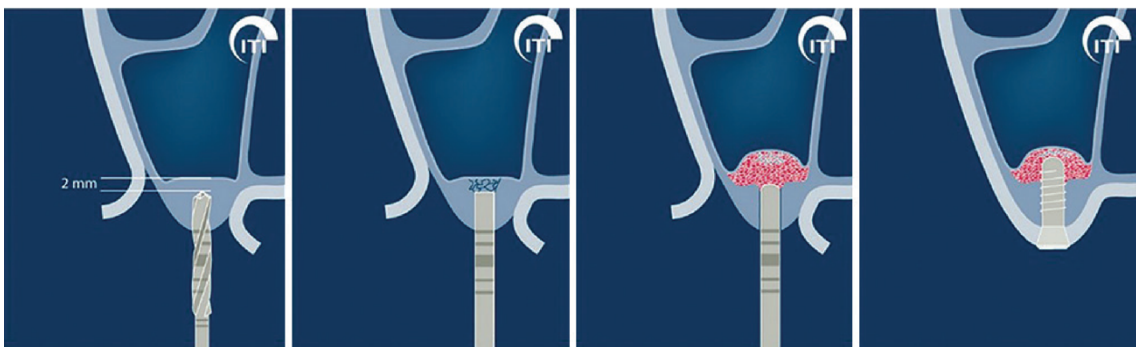


Figure 34: A crestal approach for sinus floor elevation (George et al., 2020)

The sinus lift procedure at replacing the missing bone to allow for the insertion of dental implants, exploiting the ability of bone tissue to regenerate. The graft material acts as a matrix and scaffold facilitating bone formation.

Various bone grafting materials can be used to fill the space under the elevated Schneider membrane (Kumar et al., 2013) :

- Autografts: (from the patient himself) are considered the "gold standard" due to their osteogenic, osteoconductive and osteoinductive properties. Common donor

sites include the iliac crest, mandibular symphysis (chin), anterior mandibular ramus, or maxillary tuberosity, with the choice depending on the amount of bone needed.

- Allografts: these grafts come from another individual of the same species (human). They are usually obtained from bone banks from cadavers. Allografts have both osteoconductive and osteoinductive abilities.
- Xenografts: these materials come from different species, such as beef (bovine bone mineral - BBM). Xenografts are mainly osteoconductive. Bio-Oss is a well-known example of a xenogeneic grafting material derived from bovine bone.
- Alloplastic grafts: These are synthetic or manufactured materials, derived from non-animal sources. This includes calcium phosphates, bioactive glass, and polymers.
- Growth factors: Platelet-Rich Plasma (PRP), Plasma rich in growth factors (PRGF), or Platelet-rich-fibrin (PRF). These growth factor-rich products may or may not be used in combination with biomaterial graft materials in the management of sinus lifts. PRF is considered a current trend and can improve healing and bone formation.

Some sinus lift procedures are performed without the use of exogenous graft materials. In this case, the clotted blood clot resulting from surgical bleeding fills the space under the elevated Schneider membrane (Falah et al., 2016).

CBCT is considered as an essential and highly recommended tool for the pre-operative evaluation of sinus lift procedures. It permits the evaluation of many essential anatomical parameters to guide the choice of the surgical approach such as (Rahpeyma & Khajehahmadi, 2015):

- Bone height
- Thickness of the Schneider membrane
- Presence, location, morphology and height of sinus septa
- Presence, path and diameter of the alveolar-antral artery
- Thickness of the lateral wall of the maxillary sinus
- Width and angulation of the sinus floor
- Estimating the volume of bone/biomaterial needed for the graft

III.2.3. Trans-sinus implant

The rehabilitation of the atrophic maxillary, with significant bone loss, is a challenge, especially when pneumatization of the maxillary sinus limits the insertion of implants in the posterior sectors. Various strategies exist to overcome this limitation, such as bone grafts, the use of short implants or zygomatic implants. The trans-sinus implant technique is an alternative specifically developed for the rehabilitation of the atrophic upper jaw, especially in cases where the insertion of conventional inclined implants is not possible, and before considering more complex techniques such as zygomatic implants or extended bone grafts (Maló et al., 2013).

The trans-sinus technique involves inserting the implant through the maxillary sinus to obtain an anchorage. The implant is usually angulated (often around 30 degrees from the occlusal plane), its body passes through the sinus cavity, and its apex is anchored in the bone between the anterior sinus wall and the nasal cortex (Figure 35) (Sales et al., 2024).

In order to be a viable option, it is usually necessary to have a minimum of 3-5 mm of crestal bone height for the initial anchoring of the implant head, as well as a specific anatomy of the anterior sinus wall (often described as having an 'L' or concave shape) that does not allow for the insertion of a standard angled implant entirely into the bone (Aalam et al., 2023).

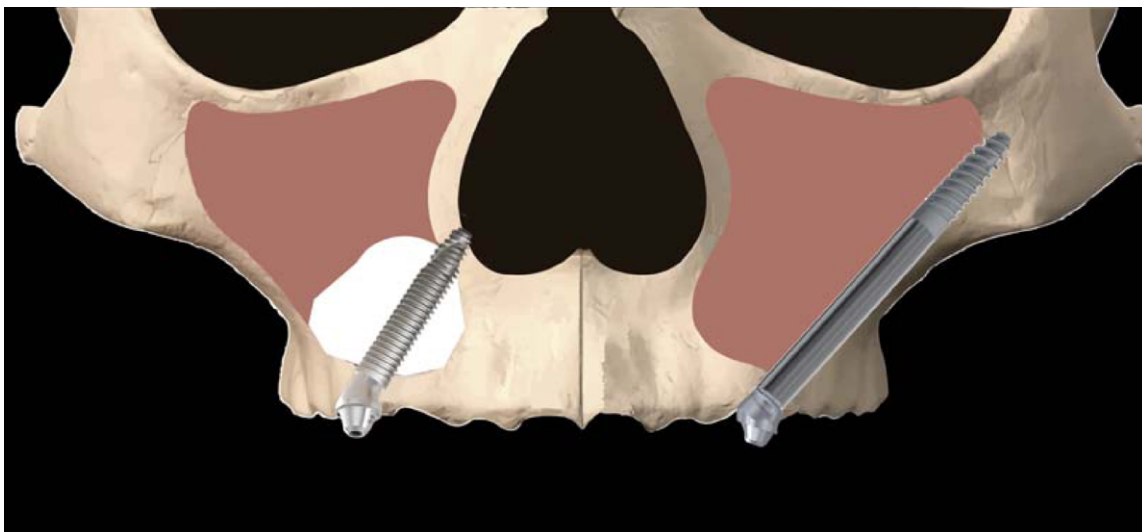


Figure 35 : Illustration of trans-sinus implant placement (left) compared to zygomatic implant placement (right) and the associated anatomy (Aalam et al., 2023)

Accurate assessment of bone anatomy is paramount in determining eligibility and planning for trans-sinus implant surgery. In this context, CBCT plays a critical role in providing crucial information for trans-sinus treatment planning (Aalam et al., 2023).

CBCT can be used to determine whether the minimum 3 to 5 mm bone height is present for the initial crestal anchorage. Visualization of the shape of the anterior sinus wall is fundamental to confirm the indication for the trans-sinus implant. A concavity or position that prevents a conventional angled implant from being fully contained within the bone is a key criterion identifiable by CBCT (Aalam et al., 2023).

CBCT is essential to evaluate the quantity and quality of bone in these regions, where the apex of the trans-sinus implant must anchor to achieve high primary stability (Maló et al., 2013). In particular, it allows the thickness of the lateral nasal wall to be measured, which is a crucial information to avoid nasal perforation during osteotomy (Aalam et al., 2023).

III.2.4. Postoperative follow-up

Postoperative follow-up is a central aspect of the management of patients who have undergone surgery or treatment for pathologies of the maxillary sinuses and surrounding maxillofacial structures. The main purpose of this follow-up is to evaluate the results of the treatment, monitor healing, detect possible complications, and monitor the recurrence of the lesions (Ruhin et al., 2005).

For tumors, rigorous follow-up is necessary, control consultations, including a radiological evaluation, are initially scheduled every quarter until the observation of homogeneous and complete bone re-ossification, then spaced out every 1 to 2 years. Radiographic control one year after enucleation attests to bone reconstruction and cortical remodeling (Ruhin et al., 2005).

Inflammatory pseudotumors of the maxillary sinus, which are rare and benign, also require postoperative clinical and radiological monitoring to check for recurrence (Ayachi et al., 2015).

For malignant tumors of the paranasal sinuses, which are often treated with surgery followed by postoperative radiotherapy, imaging is essential for the follow-up and

detection of a local or regional recurrence, MRI in this case is more useful to evaluate the extension to the soft tissues and distinguish a tumor recurrence from a simple mucosal retention (Maingon, 2001).

After surgical removal of cysts, such as extensive radiculodental cysts in the maxillary sinus, follow-up is necessary to ensure healing and manage complications such as the persistence of a fistula (Bassou et al., 2007). Follow-up may involve volumetric analysis by CBCT to assess their evolution, but it is important to correlate radiological observations with clinical symptoms to avoid overestimation (Ahmed et al., 2023).

In the context of sinus augmentation procedures, postoperative follow-up with imaging is essential to assess bone graft placement and Schneider membrane elevation (Lyu et al., 2023). It also allows for the monitoring of complications, the most common being postoperative infection or acute sinusitis (about 3% of cases). An infection can compromise the graft and requires its removal (Carrao & DeMatteis, 2015). The graft needs about 6 months to consolidate and remodel. If it is not stimulated by the placement of implants within this period, it can be resorbed. CBCT is considered a good tool for peri-implant follow-up, diagnosis of postoperative complications and their management (Jacobs & Quirynen, 2014).

Overall, CBCT is a valuable tool for post-surgical follow-up and is specifically useful for peri-implant follow-up, diagnosis and management of postoperative complications. It makes it possible to visualize anatomical structures and to detect residual or newly appeared abnormalities (Venkatesh & Venkatesh Elluru, 2017).

CONCLUSION

In summary, CBCT offers significant advantages in diagnosis and management pathologies of the maxillary sinuses. Whether in terms of visualization thanks to its superior spatial resolution, its detailed 3D image capabilities or for its radiation dose, it has revealed itself as an essential imaging technique compared to panoramic radiography and conventional CT.

Accurate assessment of maxillary sinus anatomy is crucial for the planning of surgical procedures such as implant placement, sinus floor elevations.

CBCT is now a valuable tool for the precise evaluation of maxillary sinus anatomy or post-surgical follow-up, particularly for peri-implant follow-up and the management of complications, whether for the integration of grafts after sinus floor elevations or to monitor the evolution of certain residual lesions, whether benign or malignant in nature. The integration of CBCT today has radically changed oral radiology by making it a reference imaging modality in many cases.

Even if for the evaluation of extensions of soft tissue-related pathologies or the follow-up of certain malignancies, MRI or PET scan with contrast injection may be preferable or complementary to CBCT.

However, optimizing exposure is essential nowadays, the simplest method to reduce the dose is to limit the field of view (FOV) to the region of interest only. Adequate user training is therefore necessary for minimizing redundant examinations and optimizing acquisition.

Continuous technological improvement of detectors and X-ray tubes, as well as the development of new techniques, could improve image quality and then reduce doses in the future. Artificial intelligence also shows promising potential to facilitate the diagnosis of sinus pathologies. Future research will need to continue to define the indications where CBCT outperforms others imaging techniques, particularly for soft tissue assessment.

BIBLIOGRAPHY:

- Aalam, A. A., Krivitsky-Aalam, A., Zelig, D., Oh, S., Holtzclaw, D., & Kurtzman, G. M. (2023). Trans-sinus dental implants, for immediate placement when insufficient alveolar height is present: an alternative to zygomatic implants – surgical case series. *Annals of Medicine and Surgery*, 85(1), 51–56.
<https://doi.org/10.1097/MS9.0000000000000201>
- Abramovitch, K., & Rice, D. D. (2014). Basic principles of cone beam computed tomography. In *Dental Clinics of North America* (Vol. 58, Issue 3, pp. 463–484). W.B. Saunders. <https://doi.org/10.1016/j.cden.2014.03.002>
- Ahmed, J., Gupta, A., Shenoy, N., Sujir, N., & Muralidharan, A. (2023). Prevalence of Incidental Maxillary Sinus Anomalies on CBCT Scans: A Radiographic Study. *Diagnostics*, 13(18). <https://doi.org/10.3390/diagnostics13182918>
- Ali, I. K., Parate, A. R., Fatema Shaikh Haroon, I., Kasat, V. O., & Pagare, J. S. (2015). *ROLE OF CBCT IN DIAGNOSIS OF SINONASAL CARCINOMA: CASE REPORT AND BRIEF LITERATURE REVIEW*. <https://doi.org/10.3390/jcm612011>
- Al-Okshi, A., Lindh, C., Salé, H., Gunnarsson, M., & Rohlin, M. (2015). Effective dose of cone beam CT (CBCT) of the facial skeleton: A systematic review. *British Journal of Radiology*, 88(1045). <https://doi.org/10.1259/bjr.20140658>
- Alshamrani, A. M., Mubarki, M., Alsager, A. S., Alsharif, H. K., AlHumaidan, S. A., & Al-Omar, A. (2023). Maxillary Sinus Lift Procedures: An Overview of Current Techniques, Presurgical Evaluation, and Complications. *Cureus*.
<https://doi.org/10.7759/cureus.49553>
- Arai, Y. (2021). Dmfr 50th anniversary: Review article local cone beam ct: How did it all start? In *Dentomaxillofacial Radiology* (Vol. 50, Issue 8). British Institute of Radiology. <https://doi.org/10.1259/dmfr.20210276>
- Ayachi, S., Moatemri, R., Mziou, Z., Oualha, L., Mestiri, S., & Khochtali, H. (2015). Inflammatory pseudotumor of the maxillary sinus : A case report. *Medecine Buccale Chirurgie Buccale*, 21(3), 157–162.
<https://doi.org/10.1051/mbcb/2015027>
- Bassou, D., Darbi, A., Elkharras, A., Elhaddad, A., Boumdin, H., Amil, T., Benameur, M., & Chaouir, S. (2007). Kystes radiculodentaires, une cause rare de sinus

- maxillaire opaque. *Annales d'Oto-Laryngologie et de Chirurgie Cervico-Faciale*, 124(6), 318–321. <https://doi.org/10.1016/j.aorl.2006.08.002>
- Bell, G. W., Joshi, B. B., & Macleod, R. I. (2011). Maxillary sinus disease: Diagnosis and treatment. *British Dental Journal*, 210(3), 113–118. <https://doi.org/10.1038/sj.bdj.2011.47>
- Biocanin, V. & B. D. & S. M. & T. Z. & A. M. & B. Božidar. (2015). Decompression as an effective primary approach to large radicular cyst in the maxillary sinus--A case report. *Vojnosanitetski Pregled*, 72. 634-8.
- Blanco, P., Do Pico, J. L., & Ciotta, R. (2015). Maxillary sinusitis diagnosed by ultrasound. *Medicina Intensiva*, 39(6), 391. <https://doi.org/10.1016/j.medin.2015.03.001>
- Bornstein, M. M., Horner, K., & Jacobs, R. (2017). Use of cone beam computed tomography in implant dentistry: current concepts, indications and limitations for clinical practice and research. In *Periodontology 2000* (Vol. 73, Issue 1, pp. 51–72). Blackwell Munksgaard. <https://doi.org/10.1111/prd.12161>
- Carrao, V., & DeMatteis, I. (2015). Maxillary Sinus Bone Augmentation Techniques. *Oral and Maxillofacial Surgery Clinics of North America*, 27(2), 245–253. <https://doi.org/10.1016/j.coms.2015.01.001>
- Cen, N., Sr, F., Rr, B., Oliveira Dhip, D., Fn, C., Silva, D., & Mb, S. (2020). Case Report Radiology and Diagnostic Imaging Panoramic radiography x cone beam computed tomography in surgical planning of included teeth: Series of 4 clinical cases. *Radiol Diagn Imaging*, 4, 1–5. <https://doi.org/10.15761/RDI.1000169>
- Cheong, I., Castro, V. O., Gómez, R. A., & Tamagnone, F. M. (2022). Usefulness of ultrasound in the diagnosis of nosocomial maxillary sinusitis in patients with severe Covid-19 pneumonia: a retrospective study. *Journal of Ultrasound*, 25(4), 923–927. <https://doi.org/10.1007/s40477-022-00656-5>
- Chua, E., Navaratnam, A. V., St Leger, D., Lam, V., Unadkat, S., & Weller, A. (2021). Comparison of MRI and CT in the Evaluation of Unilateral Maxillary Sinus Opacification. *Radiology Research and Practice*, 2021, 1–10. <https://doi.org/10.1155/2021/5313196>
- Conroy, D., Becht, K., Forsthoefel, M., Pepin, A. N., Lei, S., Rashid, A., Collins, B. T., Lischalk, J. W., Suy, S., Aghdam, N., Hankins, R. A., & Collins, S. P. (2021). Utilization of Iodinated SpaceOAR Vue™ During Robotic Prostate Stereotactic Body Radiation Therapy (SBRT) to Identify the Rectal–Prostate Interface and

- Spare the Rectum: A Case Report. *Frontiers in Oncology*, 10.
<https://doi.org/10.3389/fonc.2020.607698>
- Darouassi, Y., Touati, M. M., Chihani, M., Alami, J. El, Bouaity, B., & Ammar, H. (2015). Les tumeurs malignes naso-sinusiennes: À propos de 32 cas et revues de la littérature. *Pan African Medical Journal*, 22, 13–17.
<https://doi.org/10.11604/pamj.2015.22.342.8220>
- Debnath, S. C., Chishi, A. N., Nath, P., & Dhanushya, A. (2025). A Proposed Classification for Oroantral Communication to Ease the Decision-Making in Management. *Journal of Maxillofacial and Oral Surgery*.
<https://doi.org/10.1007/s12663-025-02436-0>
- Delmas, J. , R. T. , V. A. , T. J.-M. , D. P. , M. J. (2018). Anatomie des cavités nasosinusiennes. *EMC - Otolaryngology*. [https://doi.org/10.1016/s0246-0351\(17\)46938-8](https://doi.org/10.1016/s0246-0351(17)46938-8)
- Dipalma, G., Inchingolo, A. M., Trilli, I., Ferrante, L., Noia, A. Di, de Ruvo, E., Inchingolo, F., Mancini, A., Cocis, S., Palermo, A., & Inchingolo, A. D. (2025). Management of Oro-Antral Communication: A Systemic Review of Diagnostic and Therapeutic Strategies. In *Diagnostics* (Vol. 15, Issue 2). Multidisciplinary Digital Publishing Institute (MDPI). <https://doi.org/10.3390/diagnostics15020194>
- Distefano, S., Cannarozzo, M. G., Spagnuolo, G., Bucci, M. B., & Lo Giudice, R. (2023). The “Dedicated” C.B.C.T. in Dentistry. *International Journal of Environmental Research and Public Health*, 20(11).
<https://doi.org/10.3390/ijerph20115954>
- El Kettani, N. E. C., Alouat, O., El Yousfi, N., El Hassani, M. R., Chakir, N., & Jiddane, M. (2011). Kystes radiculodentaires à développement intra-sinusal maxillaire. *Feuillets de Radiologie*, 51(1), 13–16. <https://doi.org/10.1016/j.frad.2010.12.004>
- Ellis, E., & Potter, J. K. (1999). The Effects of Trauma on the Maxillary Sinus. *Oral and Maxillofacial Surgery Clinics of North America*, 11(1), 165–179.
[https://doi.org/10.1016/S1042-3699\(20\)30944-4](https://doi.org/10.1016/S1042-3699(20)30944-4)
- Eloy, P., Nollevaux, M. C., & Bertrand, B. (2005). Physiology of paranasal sinuses. In *EMC - Oto-Rhino-Laryngologie* (Vol. 2, Issue 2, pp. 185–197). Elsevier Masson SAS. <https://doi.org/10.1016/j.emcorl.2004.11.001>
- Elsayed, S. A., Alassaf, M. S., Elboraey, M. O., Mohamado, L. L., Huwaykim, D. A., Albouq, A. K., & Shahada, M. O. (2023). The Impact of Maxillary Sinus Pneumatization on the Quality of the Alveolar Bone in Dentated and Edentulous

- Patients: A Cone-Beam Computed Tomography Radiographic Analysis. *Cureus*.
<https://doi.org/10.7759/cureus.46005>
- Estrela, C., Bueno, M. R., Leles, C. R., Azevedo, B., & Azevedo, J. R. (2008). Accuracy of Cone Beam Computed Tomography and Panoramic and Periapical Radiography for Detection of Apical Periodontitis. *Journal of Endodontics*, 34(3), 273–279.
<https://doi.org/10.1016/j.joen.2007.11.023>
- Falah, M., Sohn, D. S., & Srouji, S. (2016). Graftless sinus augmentation with simultaneous dental implant placement: clinical results and biological perspectives. *International Journal of Oral and Maxillofacial Surgery*, 45(9), 1147–1153.
<https://doi.org/10.1016/J.IJOM.2016.05.006>
- Fricain, J. C. (2014). Sinusite ethmoïdo-fronto-maxillaire d'origine dentaire. In *Medecine Buccale Chirurgie Buccale* (Vol. 20, Issue 2, pp. 73–74). EDP Sciences.
<https://doi.org/10.1051/mbcb/2009037>
- Gaudy, J.-F., & Gorce, T. (2011). *Atlas d'anatomie implantaire, Chapitre 1 Situation-rapports 4 Morphologie générale 5 Sinus maxillaire Os maxillaire : morphologie et sinus maxillaire*.
- George, J., Gopal, S., Huda, F., & Thomas, N. (2020). Minimally Invasive Transalveolar Sinus Augmentation: An Answer to Sinus Conundrum. *Dentistry and Medical Research*, 8(1), 4. https://doi.org/10.4103/dmr.dmr_3_20
- Gilain, L., & Laurent, S. (2005). Maxillary sinusitis. In *EMC - Oto-Rhino-Laryngologie* (Vol. 2, Issue 2, pp. 160–173). Elsevier Masson SAS.
<https://doi.org/10.1016/j.emcorl.2004.10.005>
- Ginat, D. T., & Gupta, R. (2014). Advances in computed tomography imaging technology. In *Annual Review of Biomedical Engineering* (Vol. 16, pp. 431–453). Annual Reviews Inc. <https://doi.org/10.1146/annurev-bioeng-121813-113601>
- Göksel, S., & Güler, A. Y. (2023). Is There a Relationship Between Maxillary Sinus's Inferior Pneumatisation and Sinonasal Variations? A Retrospective CBCT Study. *Journal of Oral and Maxillofacial Research*, 14(3).
<https://doi.org/10.5037/jomr.2023.14303>
- Hallikainen, D. (1996). HISTORY OF PANORAMIC RADIOGRAPHY. *Acta Radiológica*, 37, 441–486.
- Hartmann, S. (2016). *Diagnostic ultrasound in medicine, from theory to practice HISTOIRE DE L'ÉCHOGRAPHIE*. <https://doi.org/10.1016/j>

- Hosein Kiarudi, A., Jafar Eghbal, M., Safi, Y., Mehdi Aghdasi, M., & Fazlyab, M. (2015). The Applications of Cone-Beam Computed Tomography in Endodontics: A Review of Literature. In *IEJ Iranian Endodontic Journal* (Vol. 10, Issue 1).
- Huang, Y. T., Hu, S. W., Huang, J. Y., & Chang, Y. C. (2021). Assessment of relationship between maxillary sinus membrane thickening and the adjacent teeth health by cone-beam computed tomography. *Journal of Dental Sciences*, *16*(1), 275–279. <https://doi.org/10.1016/j.jds.2020.05.002>
- Hung, K., Hui, L., Yeung, A. W. K., Wu, Y., Hsung, R. T. C., & Bornstein, M. M. (2021). Volumetric analysis of mucous retention cysts in the maxillary sinus: A retrospective study using cone-beam computed tomography. *Imaging Science in Dentistry*, *51*, 1–11. <https://doi.org/10.5624/isd.20200267>
- Iwanaga, J., Wilson, C., Lachkar, S., Tomaszewski, K. A., Walocha, J. A., & Tubbs, R. S. (2019). Clinical anatomy of the maxillary sinus: Application to sinus floor augmentation. *Anatomy and Cell Biology*, *52*(1), 17–24. <https://doi.org/10.5115/acb.2019.52.1.17>
- Jacobs, R., & Quirynen, M. (2014). Dental cone beam computed tomography: Justification for use in planning oral implant placement. *Periodontology 2000*, *66*(1), 203–213. <https://doi.org/10.1111/prd.12051>
- Jankowski, R., Nguyen, D. T., Poussel, M., Chenuel, B., Gallet, P., & Rumeau, C. (2016). Sinusology. In *European Annals of Otorhinolaryngology, Head and Neck Diseases* (Vol. 133, Issue 4, pp. 263–268). Elsevier Masson SAS. <https://doi.org/10.1016/j.anorl.2016.05.011>
- Jawahar, A. (2021). Maxillary Sinus Pathologies In Orthopantomography. *Int J Dentistry Oral Sci*, *8*(8), 3738–3742. <https://scidoc.org/IJDOS.php>
- Jung, Y. H., & Cho, B. H. (2012). Assessment of the relationship between the maxillary molars and adjacent structures using cone beam computed tomography. *Imaging Science in Dentistry*, *42*(4), 219–224. <https://doi.org/10.5624/isd.2012.42.4.219>
- Kamina. (2009). *Anatomie Clinique Tome 2 : Os de la Face - Cavités et Os de la Tête Osseuse*.
- Kang, S. H., Kim, B. S., & Kim, Y. (2015). Proximity of posterior teeth to the maxillary sinus and buccal bone thickness: A biometric assessment using cone-beam computed tomography. *Journal of Endodontics*, *41*(11), 1839–1846. <https://doi.org/10.1016/j.joen.2015.08.011>

- Karantanas, A. H., & Sandris, V. (1997). Maxillary sinus inflammatory disease: Ultrasound compared to computed tomography. *Computerized Medical Imaging and Graphics*, 21(4), 233–241. [https://doi.org/10.1016/S0895-6111\(97\)00015-3](https://doi.org/10.1016/S0895-6111(97)00015-3)
- Khandelwal, P., & Hajira, N. (2017). Management of Oro-antral Communication and Fistula: Various Surgical Options. *World Journal of Plastic Surgery*, 6(1), 3–8. www.wjps.ir
- Kiljunen, T., Kaasalainen, T., Suomalainen, A., & Kortenesniemi, M. (2015). Dental cone beam CT: A review. In *Physica Medica* (Vol. 31, Issue 8, pp. 844–860). Associazione Italiana di Fisica Medica. <https://doi.org/10.1016/j.ejmp.2015.09.004>
- Kiran Kumar, N., Merwade, S., Prabakaran, P., C H, L. P., B S, A., & C N, G. (2021). Magnetic resonance imaging versus cone beam computed tomography in diagnosis of periapical pathosis – A systematic review. In *Saudi Dental Journal* (Vol. 33, Issue 8, pp. 784–794). Elsevier B.V. <https://doi.org/10.1016/j.sdentj.2021.09.010>
- Klossek, J. M., Quinet, B., Bingen, E., François, M., Gaudelus, J., Larnaudie, S., Liard, F., Péan, Y., Roger, G., Reveillaud, O., & Serrano, E. (2007). État actuel de la prise en charge des infections rhinosinusiennes aiguës de l'enfant en France. In *Medecine et Maladies Infectieuses* (Vol. 37, Issue 3, pp. 127–152). <https://doi.org/10.1016/j.medmal.2006.11.008>
- Kumar, P., Vinitha, B., & Fathima, G. (2013). Bone grafts in dentistry. In *Journal of Pharmacy and Bioallied Sciences* (Vol. 5, Issue SUPPL.1). <https://doi.org/10.4103/0975-7406.113312>
- Kunzendorf, B., Naujokat, H., & Wiltfang, J. (2021). Indications for 3-D diagnostics and navigation in dental implantology with the focus on radiation exposure: a systematic review. *International Journal of Implant Dentistry*, 7(1). <https://doi.org/10.1186/s40729-021-00328-9>
- Lacević, & Vranić, E. (2004). *DIFFERENT DIGITAL IMAGING TECHNIQUES IN DENTAL PRACTICE*. <https://doi.org/https://doi.org/10.17305/bjbms.2004.3412>
- Langlais, R. P., Mah, P., & Goulet, J. P. (2009). The contribution of Cone-Beam CT in the assessment of orofacial pain. In *Douleur et Analgesie* (Vol. 22, Issue 2, pp. 112–120). Springer Paris. <https://doi.org/10.1007/s11724-009-0132-9>
- Li, G. (2013). Patient radiation dose and protection from cone-beam computed tomography. *Imaging Science in Dentistry*, 43(2), 63–69. <https://doi.org/10.5624/isd.2013.43.2.63>

- Lyu, M., Xu, D., Zhang, X., & Yuan, Q. (2023). Maxillary sinus floor augmentation: a review of current evidence on anatomical factors and a decision tree. In *International Journal of Oral Science* (Vol. 15, Issue 1). Springer Nature. <https://doi.org/10.1038/s41368-023-00248-x>
- M. De Marneffe (1), M. M. (2), M. M. (3). (2017). *Cone Beam CT Nouvel outil dans l'imagerie diagnostique*.
- MacDonald, D., & Telyakova, V. (2024). An Overview of Cone-Beam Computed Tomography and Dental Panoramic Radiography in Dentistry in the Community. In *Tomography* (Vol. 10, Issue 8, pp. 1222–1237). Multidisciplinary Digital Publishing Institute (MDPI). <https://doi.org/10.3390/tomography10080092>
- MacDonald-Jankowski, D. S., & Orpe, E. C. (2006). Computed tomography for oral and maxillofacial surgeons. Part 2: Cone-beam computed tomography. *Asian Journal of Oral and Maxillofacial Surgery*, 18(2), 85–92. [https://doi.org/10.1016/S0915-6992\(06\)80001-4](https://doi.org/10.1016/S0915-6992(06)80001-4)
- Maia Nobre Rocha de Miranda, C., Pontes de Miranda Maranhão, C., Maia Nobre Rocha Arraes, F., Gomes Padilha, I., de Pádua Gomes de Farias, L., Stephanie de Araujo Jatobá, M., Carolina Mendonça de Andrade, A., & Gomes Padilha, B. (2011). Anatomical variations of paranasal sinuses at multislice computed tomography: what to look for*. In *Jul/Ago* (Vol. 44, Issue 4).
- Maingon, P. (2001). *Les tumeurs des sinus de la face*.
- Maló, P., Nobre, M. de A., & Lopes, A. (2013). Immediate loading of “All-on-4” maxillary prostheses using trans-sinus tilted implants without sinus bone grafting: a retrospective study reporting the 3-year outcome. *European Journal of Oral Implantology*, 6(3), 273–283. <https://pubmed.ncbi.nlm.nih.gov/24179981/>
- Matern, J. F., Keller, P., Carvalho, J., Dillenseger, J. P., Veillon, F., & Bridonneau, T. (2016). Radiological sinus lift: A new minimally invasive CT-guided procedure for maxillary sinus floor elevation in implant dentistry. *Clinical Oral Implants Research*, 27(3), 341–347. <https://doi.org/10.1111/clr.12549>
- Mclaren, D. L., Hospital, O., Lenkeit, C. P., Lofgren, D. H., Carl, ;, & Affiliations, S. (2020). *Maxillary Sinus Fracture*. <https://www.ncbi.nlm.nih.gov/books/NBK557455/?report=printable>
- Mladina, R., Risavi, R., Branica, S., & Heinzl, B. (1994). *A-mode diagnostic ultrasound of maxillary sinuses: Possibilities and limitations*t* (Vol. 32).

- Mortazavi, S., Khadem-Reza, Z. K., & Parvaresh, M. (2024). Investigation of the effect of field of view on the amount of dental implant artifacts in cone beam computed tomography images. *Egyptian Journal of Radiology and Nuclear Medicine*, 55(1). <https://doi.org/10.1186/s43055-024-01274-3>
- Mularczyk, C., & Welch, K. (2024). Maxillary Sinus Anatomy and Physiology. In *Otolaryngologic Clinics of North America*. W.B. Saunders. <https://doi.org/10.1016/j.otc.2024.07.004>
- Norton, N. S. (2011). *Netter's Head and Neck Anatomy for Dentistry* (Elsevier / Saunders, Ed.; 2nd edition). <https://doi.org/https://doi.org/10.1038/sj.bdj.2012.517>
- Oberli, K., Bornstein, M. M., & von Arx, T. (2007). Periapical surgery and the maxillary sinus: radiographic parameters for clinical outcome. *Oral Surgery, Oral Medicine, Oral Pathology, Oral Radiology and Endodontology*, 103(6), 848–853. <https://doi.org/10.1016/j.tripleo.2006.09.017>
- Oishi, S., Ishida, Y., Matsumura, T., Kita, S., Sakaguchi-Kuma, T., Imamura, T., Ikeda, Y., Kawabe, A., Okuzawa, M., & Ono, T. (2020). A cone-beam computed tomographic assessment of the proximity of the maxillary canine and posterior teeth to the maxillary sinus floor: Lessons from 4778 roots. *American Journal of Orthodontics and Dentofacial Orthopedics*, 157(6), 792–802. <https://doi.org/10.1016/j.ajodo.2019.06.018>
- Olszewski, R. (2020). Artifacts related to cone beam computed tomography technology (CBCT) and their significance for clinicians: illustrated review of medical literature. *NEMESIS*, 11(1), 1–29. <https://doi.org/10.14428/nemesis.v11i1.54393>
- Pauwels, R., Araki, K., Siewerdsen, J. H., & Thongvigitmanee, S. S. (2015). Technical aspects of dental CBCT: State of the art. In *Dentomaxillofacial Radiology* (Vol. 44, Issue 1). British Institute of Radiology. <https://doi.org/10.1259/dmfr.20140224>
- Pommer, B. (2012). *The percrestal sinus lift from illusion to reality : Chapter 1 : Maxillary sinus anatomy and physiology* (Georg Watzek, Ed.; Quintessence). <https://www.researchgate.net/publication/279189432>
- Premoli Maciel, A., Albano Lopes, I., Adami Tucunduva, R. M., Simpione, G., Da Silva Santos, P. S., Damante, J. H., & Alvares Capelozza, A. L. (2020). Contribution of the CBCT in the diagnosis and treatment plan of odontogenic maxillary sinusitis: Cases Reports. *Revista Estomatológica Herediana*, 30(1), 47–52. <https://doi.org/10.20453/reh.v30i1.3740>

- Psillas, G., Papaioannou, D., Petsali, S., Dimas, G. G., & Constantinidis, J. (2021). Odontogenic maxillary sinusitis: A comprehensive review. *Journal of Dental Sciences*, 16(1), 474–481. <https://doi.org/10.1016/J.JDS.2020.08.001>
- Rahpeyma, A., & Khajehahmadi, S. (2015). Open Sinus Lift Surgery and the Importance of Preoperative Cone-Beam Computed Tomography Scan: A Review. In *Journal of International Oral Health* (Vol. 7, Issue 9).
- Regnstrand, T., Torres, A., Petitjean, E., Lambrechts, P., Benchimol, D., & Jacobs, R. (2021). CBCT-based assessment of the anatomic relationship between maxillary sinus and upper teeth. *Clinical and Experimental Dental Research*, 7(6), 1197–1204. <https://doi.org/10.1002/cre2.451>
- Ruhin, B., Guilbert, F., & Bertrand, J. C. (2005). Treatment of maxillary and mandibular cysts and benign tumours. In *EMC-Stomatologie* (Vol. 1, Issue 1, pp. 42–59). Elsevier Masson SAS. <https://doi.org/10.1016/j.emcsto.2005.01.003>
- Rushton, V. E., & Horner, K. (1996). The use of panoramic radiology in dental practice. In *Journal of Dentistry* (Vol. 24, Issue 3).
- Sales, P. H. da H., Diniz, D. A., Silva, P. G. de B., Carvalho, A. de A. T., Vescovi, P., Meleti, M., & Leão, J. C. (2024). Effectiveness of trans-sinus dental implants in the complete arch rehabilitation of the edentulous maxilla: A systematic review and meta-analysis. *The Journal of Prosthetic Dentistry*. <https://doi.org/10.1016/J.PROSDENT.2024.08.003>
- Sayáns, M. P., Suárez Quintanilla, J. A., Chamorro Petronacci, C. M., Suárez Peñaranda, J. M., Jornet, P. L., García, F. G., & Sánchez, Y. G. (2020). Volumetric study of the maxillary sinus in patients with sinus pathology. *PLoS ONE*, 15(6). <https://doi.org/10.1371/journal.pone.0234915>
- Shahrou, R., Sha, P., Withana, T., Jun, J., & Sye, A. Z. (2021). Oroantral communication, its causes, complications, treatments and radiographic features: A pictorial review. *Imaging Science in Dentistry*, 51, 1–5. <https://doi.org/10.5624/ISD.20210035>
- Shin, H. S., Nam, K. C., Park, H., Choi, H. U., Kim, H. Y., & Park, C. S. (2014). Effective doses from panoramic radiography and CBCT (cone beam CT) using dose area product (DAP) in dentistry. *Dentomaxillofacial Radiology*, 43(5). <https://doi.org/10.1259/dmfr.20130439>
- Simonds, J. S., Whitlow, C. T., Chen, M. Y. M., & Williams, D. W. (2011). Isolated fractures of the posterior maxillary sinus: CT appearance and proposed

- mechanism. *American Journal of Neuroradiology*, 32(3), 468–470.
<https://doi.org/10.3174/ajnr.A2337>
- Sumathy, G., & Muthiah, S. (2020). Odontogenic Maxillary Sinusitis. *European Journal of Molecular & Clinical Medicine*, 07(10).
<https://www.researchgate.net/publication/358996143>
- Suparno, N. R., Faizah, A., & Nafisah, A. N. (2023). Assessment of Panoramic Radiograph Errors: An Evaluation of Patient Preparation and Positioning Quality at Soelastri Dental and Oral Hospital. *The Open Dentistry Journal*, 17(1).
<https://doi.org/10.2174/0118742106261974230925073155>
- Tilaveridis, I., Stefanidou, A., Kyrgidis, A., Tilaveridis, S., Tilaveridou, S., & Zouloumis, L. (2022). Foreign bodies of dental iatrogenic origin displaced in the maxillary sinus - A safety and efficacy analysis of a retrospective study. *Annals of Maxillofacial Surgery*, 12(1), 33–38. https://doi.org/10.4103/ams.ams_190_21
- Vacher, C. (2013). Bases anatomiques de l’abord du sinus maxillaire pour l’implantologie. *Actualités Odonto-Stomatologiques*, 265, 19–23.
<https://doi.org/10.1051/aos/2013503>
- Valente, N. A. (2016). Anatomical Considerations on the Alveolar Antral Artery as Related to the Sinus Augmentation Surgical Procedure. In *Clinical implant dentistry and related research* (Vol. 18, Issue 5, pp. 1042–1050). John Wiley and Sons Inc. <https://doi.org/10.1111/cid.12355>
- Venkatesh, E., & Venkatesh Elluru, S. (2017). CONE BEAM COMPUTED TOMOGRAPHY: BASICS AND APPLICATIONS IN DENTISTRY. *Journal of Istanbul University Faculty of Dentistry*, 51(0).
<https://doi.org/10.17096/jiufd.00289>
- White, S. C., & Pharoah, M. J. (2008). The Evolution and Application of Dental Maxillofacial Imaging Modalities. In *Dental Clinics of North America* (Vol. 52, Issue 4, pp. 689–705). <https://doi.org/10.1016/j.cden.2008.05.006>
- Whyte, A., & Boeddinghaus, R. (2019). The maxillary sinus: Physiology, development and imaging anatomy. *Dentomaxillofacial Radiology*, 48(8).
<https://doi.org/10.1259/dmfr.20190205>
- Yeung, A. W. K., Hung, K. F., Li, D. T. S., & Leung, Y. Y. (2022). The Use of CBCT in Evaluating the Health and Pathology of the Maxillary Sinus. In *Diagnostics* (Vol. 12, Issue 11). Multidisciplinary Digital Publishing Institute (MDPI).
<https://doi.org/10.3390/diagnostics12112819>

- Yeung, A. W. K., Tanaka, R., Khong, P. L., von Arx, T., & Bornstein, M. M. (2018). Frequency, location, and association with dental pathology of mucous retention cysts in the maxillary sinus. A radiographic study using cone beam computed tomography (CBCT). *Clinical Oral Investigations*, 22(3), 1175–1183. <https://doi.org/10.1007/s00784-017-2206-z>